SSD

SCIENCE FOR A SUSTAINABLE DEVELOPMENT

FINAL REPORT PHASE I

ADVANCED EXPLOITATION OF GROUND-BASED MEASUREMENTS FOR ATMOSPHERIC CHEMISTRY AND CLIMATE APPLICATIONS

«AGACC»

M. DE MAZIERE, H. DE BACKER, M. CARLEER, E. MAHIEU,
P. DEMOULIN, P. DUCHATELET, A. CHEYMOL, K. CLEMER, P.F. COHEUR, B. DILS, S. FALLY,
F. HENDRICK, C.HERMANS, M. KRUGLANSKI, A. MANGOLD, J. VANDER AUWERA,
R. VAN MALDEREN, M. VAN ROOZENDAEL, C. VIGOUROUX

ENERGY

TRANSPORT AND MOBILITY

AGRO-FOOD

HEALTH AND ENVIRONMENT

CLIMATE

BIODIVERSITY

ATMOSPHERE AND TERRESTRIAL AND MARINE ECOSYSTEMS

TRANSVERSAL ACTIONS

.be

SCIENCE FOR A SUSTAINABLE DEVELOPMENT
(SSD)

Atmosphere

FINAL REPORT PHASE 1

ADVANCED EXPLOITATION OF GROUND-BASED MEASUREMENTS FOR ATMOSPHERIC CHEMISTRY AND CLIMATE APPLICATIONS «AGACC»

SD/AT/01A

Promotors

Martine De Mazière
Belgisch Instituut voor Ruimte Aeronomie (BIRA-IASB)
Ringlaan 3 – 1180 Brussel
Tel: 02/373.03.63 - Fax: 02/374.84.23
martine.demaziere@aeronomie.be

Hugo De Backer
Koninklijk Meteorologisch Instituut van België (KMI-IRM)

Michel Carleer
Université Libre de Bruxelles (ULB) – Service de Chimie Quantique et Photophysique (SCQP)

Emmanuel Mahieu
Institute of Astrophysics and Geophysics
University of Liège (ULg)
Groupe Infra-Rouge de Physique Atmosphérique et Solaire (GIRPAS)

Authors

Martine De Mazière
with contributions from

K. Clemer, B. Dils, F. Hendrick, C. Hermans,
M. Kruglanski, M. Van Roozendael, C. Vigouroux
BIRA-IASB
A. Cheymol, H. De Backer, A. Mangold, R. Van Malderen
KMI-IRM
M. Carleer, P.F. Coheur, S. Fally, J. Vander Auwera
ULB
P. Demoulin, P. Duchatelet, E. Mahieu
ULg

BELGIAN SCIENCE POLICY

Rue de la Science 8
Wetenschapsstraat 8
B-1000 Brussels
Belgium
Tel: +32 (0)2 238 34 11 – Fax: +32 (0)2 230 59 12
http://www.belspo.be

Contact person:
Mrs Martine Vanderstraeten : +32 (0)2 238 36 10
Project Website: http://www.oma.be/AGACC/Home.html

M. De Mazière, H. De Backer, M. Carleer, E. Mahieu, P. Demoulin, P. Duchatelet, A. Cheymol, K. Clemer, PF. Coheur, B. Dils, S. Fally, F. Hendrick, C. Hermans, M. Kruglanski, A. Mangold, J. Vander Auwera, R. Van Malderen, M. Van Roozendael, C. Vigouroux, ***Advanced exploitation of ground-based measurements for atmospheric chemistry and climate applications «AGACC»***. Final Report Phase 1. Brussels : Belgian Science Policy 2009 – 51 p. (Research Programme Science for a Sustainable Development)

TABLE OF CONTENTS

1 SUMMARY

The AGACC project (Advanced exploitation of Ground-based measurements for Atmospheric Chemistry and Climate applications) joins international scientific research regarding important environmental issues, that are our changing climate and degrading air quality. There is evidence for a strong link between the chemical composition of the atmosphere – including the troposphere and the stratosphere - and climate. Air quality is dominated by the boundary layer and lower troposphere composition, and the underlying emissions. AGACC therefore exploits past and current ground-based observations at Ukkel (50.5°N, 4°E), Jungfraujoch (ISSJ, 46.5°N, 8°E) and Ile de La Réunion (21°S, 55°E) for investigating chemical changes in the atmosphere that have an impact on the Earth's climate and/or air quality. In particular, it targets the detection and quantification of a number of atmospheric constituents that hitherto have not been looked at in depth, because they require advanced detection methods.

Various such advanced detection techniques are mastered in the AGACC consortium. Moreover, a good synergy between the various observation methods exists and is exploited in the project, as will be demonstrated in this report. It must also be mentioned that AGACC benefits from the international community in which the partners are involved – in particular the Network for the Detection of Atmospheric Composition Change (NDACC) and the COST Action WAVACS (Atmospheric Water Vapour and the Climate System; Action ES0604) that started in 2007.

The project is structured according to a number of activities and workpackages: the particular objectives of these are given hereafter, together with the associated results obtained thus far in the first phase of the project (2006-April 2008).

<u>WP1000 Atmospheric Water Vapour</u>

Water vapour is the most important greenhouse gas. There are indications that the amount of water vapour is changing. More investigations are needed to elucidate these changes and their origin. WAVACS is an example of the attention that is currently given on the international scene to this constituent. One of the major challenges is the measurement of water vapour in the upper troposphere / lower stratosphere, where large vertical gradients exist. Another complication is the fact that the abundance of water vapour is highly variable, in time and space. The determination of the water vapour isotopologues can shed light on the processes that underly its distribution in the atmosphere.

Remote sensing using Fourier transform infrared (FTIR) spectrometry is a candidate method to determine these isotopologues. Retrieval strategies for determining the amount and vertical distribution of the atmospheric water vapour above Uccle, Jungfraujoch and Ile de La Reunion from FTIR observations have been developed. Promising results have been obtained at all sites, for the primary as well as for some secondary isotopologues ($H_2{}^{16}O$, $H_2{}^{18}O$, HDO). Comparisons with the IASI satellite data, although very preliminary, demonstrated the complementarity of both datasets and the need for joint retrievals. The accurate detection of water vapour by FTIR must be pursued because the FTIR technique has the potential to record isotopologues amounts and isotopic ratios on a continuous basis, and therefore to provide valuable information about transport and dynamical processes. At Ukkel, profiles (up to about 8 to 12 km altitude) and integrated water vapour amounts have been compared with several other instruments (radiosoundings, CIMEL data, GPS measurements). The observed biases are always smaller than 20%. The investigation of the discrepancies will be pursued, and optimal retrieval strategies will be defined.

At Ukkel, a timeseries of radiosoundings exists going back to 1990. It is known that such measurements are indebted with a number of artefacts. The Leiterer method (2005) has been found to be the better method to correct for these artefacts. After its application to the Uccle soundings, preliminary trends for the relative humidity in the upper troposphere and at the tropopause have been determined. We observe an increasing humidity before 2001 at a rate of 0.97%/year and a strong decrease since then, by -3.57%/year. These changes seem to be

caused by a lifting, respectively lowering of the tropopause The causes for these changes are not yet understood. .
Further work will include the investigation of temporal and spatial variabilities of the atmospheric water vapour abundance.

WP 1200 Aerosol

The CIMEL instrument was installed at Uccle (50.5°N, 4°E) in summer 2006. The sunphotometer operated correctly from July 2006 until September 2007. During the time period October 2007-Februari 2008 the instrument was recalibrated at Carpentras (44° N, 5° E). Since March 2008 the recalibrated sunphotometer is fully operational again. The processed data, e.g., aerosol optical depth (AOD), aerosol size distribution, and integrated water vapor (IWV), are available on the AERONET website (http://aeronet.gsfc.nasa.gov/), and have been used in several studies since then, among which a comparison with aerosol data derived from the Brewer instrument at Uccle.
A new MAXDOAS instrument has been built, with a configuration that is optimised for enabling the determination of aerosol optical depth and optical properties. It allows the collection of scattered solar light, as well as direct sun measurements using a sun tracker. First tests of the instrument at Uccle are ongoing. A first version of an aerosol inversion algorithm for the MAXDOAS spectra has been developed. It has the capability to retrieve aerosol extinction vertical profiles and total aerosol optical depths based on measurements of the O_4 slant column densities (using the DOAS technique) and relative changes in intensities. An important improvement of this algorithm compared to previously reported retrieval algorithms, is the implementation of the radiative transfer code LIDORT in the forward model. This enables an analytical calculation of the weighting functions. The Optimal Estimation Method has been implemented to solve the inverse problem. The algorithm has been tested successfully on simulated spectra: it looks like one obtains a number of degrees of freedom for the aerosol retrieval around 4. The algorithm will soon be verified on real spectra, and the results will be compared with CIMEL and Brewer data.

WP 1300 Climate gases

Formaldehyde (H_2CO) is one of the most abundant carbonyl compounds and a central component of the oxidation of volatile organic compounds (VOC). It represents the total amount of oxidized VOC. Its observation can help to constrain VOCs emissions in models and supports air quality control regulations. Both NOx and VOC concentrations determine the production of ozone in the troposphere, a climate gas. Sources of H_2CO are methane oxidation (background), biogenic VOCs oxidation (isoprene), anthropogenic hydrocarbon oxidation, and biomass burning. Sinks are oxidation by OH radical and photolysis. H_2CO is a major source of CO.
Strategies have been developed to retrieve H_2CO from MAXDOAS spectra and from FTIR spectra, above Uccle and Ile de La Réunion. The MAXDOAS and FTIR inversion results for the tropospheric columns of H_2CO agree very well in capturing the diurnal, daily and seasonal variabilities. There is also good agreement with correlative GOME or SCIAMACHY data, retrieved independently using a DOAS technique. A small bias observed between MAXDOAS or SCIAMACHY satellite data and FTIR columns probably has its origin in spectroscopic uncertainties. At Jungfraujoch, where the H_2CO columns are about a factor 4 smaller than at Reunion Island, a special detection setup has lead to reliable results. Timeseries between Dec. 2005 and February 2007 show a distinct seasonal variation with a minimum in local winter. Work is ongoing to confront the observational data with IMAGES model simulations.
Methane (CH_4) is the third most important greenhouse gas, after H_2O and CO_2. Information about its isotopologues may provide indications for the origin and age of the sampled airmass.
Several successful retrieval strategies for the detection of $^{13}CH_4$ have been developed at Jungfraujoch, and have been compared among them. The recommended strategy uses 1 microwindow in the MCT detector range, and provides a good sensitivity up to 14 km altitude.
Retrievals of CH_3D are more difficult, because there are strong interferences with water vapour. Two successful retrieval strategies have been developed at Jungfraujoch. One of them, the multiwindow strategy, has already been verified successfully at Reunion Island for spectra taken at large solar zenith angles, despite very significant interferences with water vapour absorptions.

The thus derived isotopic ratio δD appears to behave as expected. The second one, the multi-spectra strategy, will be investigated next.
It has also been possible to retrieve timeseries of hydrogen cyanide (HCN) column abundances at Jungfraujoch, using a strategy fitting simultaneously five HCN lines In the 3260-3310 cm^{-1} spectral region. The main HCN source is believed to be biomass burning, making this species a useful tracer of fires. Oxidation by the OH radical is among the identified sinks, while uptake by oceans has been hypothesized as the dominant removal process. The Jungfraujoch timeseries shows a strong feature due to the advection of biomass burning products in 1998. The comparison of the retrieved time series of partial columns between 7 and 20 km altitude above Jungfraujoch with correlative ACE-FTS partial columns show excellent agreement. In particular the seasonal variation, with a maximum in July, is observed identically in both timeseries. More work is needed to retrieve HCN at Ile de La Réunion, due to stronger interferences with water vapour.
Acetylene (C_2H_2) is among the nonmethane hydrocarbons (NMHCs) accessible to the FTIR remote sensing technique. As a product of combustion and biomass burning, it is emitted at the Earth surface and further transported and mixed into the troposphere. Destruction by OH is the main removal process. We have demonstrated that acetylene can be retrieved from FTIR spectra at Jungfraujoch using four lines close to 3251, 3255, 3278 and 3305 cm^{-1}. The timeseries of tropospheric columns above Jungfraujoch allows to characterize the strong seasonal variation of C_2H_2, with maximum columns generally observed around mid-February. On average, the peak-to-peak amplitude of the seasonal variation amounts to nearly 90% of the mean yearly column. The enhancement of HCN due to biomass burning that was observed in 1998, is well correlated with that observed in the C_2H_2 timeseries, as well as with the corresponding data for CO and C_2H_6. Comparisons between timeseries of partial columns between 7 and 17 km altitude from the ground-based FTIR and the satellite ACE-FTS instruments show a reasonable agreement, although the latter seems to be slightly biased high, especially during summertime. At present, the comparison covers the period early 2004 to the end of 2007. An extension in time of the ACE-FTS data set is needed to confirm these first conclusions.

WP 1400 Feasibility studies

Ethylene (C_2H_4) originates from a variety of anthropogenic (e.g. cars in urban areas) and natural (e.g. plants, volcanoes, forest fires) sources., It is difficult to detect C_2H_4 from FTIR spectra, due to its very short chemical lifetime, and in particular at the high-altitude remote site of the Jungfraujoch. However, we have demonstrated that it is possible to clearly detect larger absorptions of ethylene in Jungfraujoch FTIR spectra recorded during special events, e.g. under enhanced biomass burning, when the column is about 4 times larger than the average one.
Other feasibility studies have been initiated, looking at absorptions of HCFC-142b (CH_3CClF_2) in Jungfraujoch low sun spectra. Several retrieval strategies are under test.

WP 2000 - ACQUISITION AND EXPLOITATION OF SUPPORTING DATA

Laboratory spectroscopic measurements in support of the analysis of atmospheric spectra have been continued. The focus has been on water vapour and its isotopologues, the 9 micron region of the formic acid (H_2CO_2) absorptions and the 1–0 band of $^{13}C^{16}O$ near 2096 cm^{-1}.
Linelists of HDO (11500-23000 cm^{-1}) and D_2O (8800-9520 cm^{-1}) have been generated. Also, the experimental linelists of HDO and D_2O that cover the wide 5600-11600 cm^{-1} region have been built. They contain line positions, intensities, self- and air-broadening coefficients, and air-induced shifts and their statistical uncertainties. In the near-IR spectral region (4200-6600 cm^{-1}), a complete linelist has been produced for the $H_2{}^{16}O$, $H_2{}^{17}O$, $H_2{}^{18}O$ and HDO isotopologues. It is accessible to the scientific community through the web (http://www.ulb.ac.be/cpm). The water vapour continuum underlying the discrete lines is under investigation.
A new database for the 9 micron region of the formic acid spectrum was generated: it is now provided as an update to the HITRAN database and will be included in the forthcoming version of GEISA.
Our results for the line intensities of $^{13}C^{16}O$ are on average 1.5 % higher than those available for these lines in the HITRAN database, characterized by a 2–5 % accuracy. This is an

excellent agreement, indicating that the accuracy of 1–0 band $^{13}C^{16}O$ line intensities in HITRAN is probably close to 2 %.
As seen above, our investigations have made use of ancillary and complementary data wherever useful.

WP 3000 Valorisation of the results.

The results have been presented at many occasions at international Symposia, and at the yearly NDACC UV-Vis and Infrared Working Group Meetings, and a number of refereed publications have already appeared. We expect much benefit also from the COST Action WAVACS. The laboratory results have been or will be integrated in the international spectroscopic databases HITRAN and GEISA. Our expertise is also recognized through our participation to European projects like SCOUT-O3, GEOmon and HYMN.

2 INTRODUCTION

2.1 Context

The evolution of our environment, in particular climate and air quality, will have important socio-economic and health consequences. Better knowledge of this evolution and of the atmospheric processes involved will lead to more accurate prediction capabilities and thus allow policy makers to prepare knowledge-based adaptation and mitigation strategies. There is evidence for a strong link between the chemical composition of the atmosphere – including the troposphere and the stratosphere - and climate. Air quality is dominated by the boundary layer and lower troposphere composition, and the underlying emissions. Therefore, AGACC joins international scientific research regarding these issues, as it will exploit past and current ground-based observations for investigating chemical changes in the atmosphere that have an impact on the Earth's climate or air quality. In particular, it targets the detection and quantification of a number of atmospheric constituents that hitherto have not been looked at in depth, because they require advanced detection methods.

2.2 Objectives and expected outcomes

The general objectives of the project are to derive new and improved data sets for the target geophysical parameters. These are lower tropospheric aerosols, water vapour in the troposphere and lower stratosphere, as well as methane and HCFCs; they have a direct impact on climate. Also a number of source gases (CO, HCN, H_2CO) that influence the cleaning capacity of the atmosphere, and therefore tropospheric chemistry, air quality and indirectly also climate, will be studied. Some feasibility studies are planned for the detection of isotopologues of CH_4, CO and water (e.g., HDO): the isotopic composition allows one to distinguish between possible sources of the species. It will be investigated whether OH and C_2H_4 (ethylene), for which only few data exist, can be detected.
The partners, having complementary ground-based instrumentation and associated expertises, have joined their forces to exploit at best the synergies between the various observation techniques in order to reach the objectives. The instruments involved are Fourier transform infrared (FTIR), UV-Visible Multi-Axis Differential Optical Absorption Spectroscopy (MAXDOAS), and Brewer spectrometers, and a sun photometer, deployed at Ukkel (50.5°N, 4°E), Jungfraujoch (ISSJ, 46.5°N, 8°E) and Ile de La Réunion (21°S, 55°E).
AGACC will deliver original and advanced datasets for the target parameters. It will characterize evolutions of greenhouse gases and of relevant related species at Ukkel and ISSJ. Examples are the time series and trends of relative humidity, and of aerosol load and surface radiation at Ukkel, or the evolution of CH_4 and its isotopic partitioning above ISSJ. The aerosol results will enable the generation and dissemination of an improved UV-index prediction for Ukkel. AGACC will also provide an inventory of new HCFC/HFC compounds presenting infrared absorption features in ISSJ spectra, and an assessment of the feasibility to retrieve water vapour and some other target gases from FTIR spectra at the various sites. New data will be collected at Ile de La Réunion.
In addition, new laboratory spectroscopic data will be provided and submitted to the relevant databases that are HITRAN and GEISA.
The project will also care for a proper interpretation and dissemination of the research results, e.g., in the satellite community, which is very eager to get support from ground-based investigations, for example for the detection of H_2CO. ULg, BIRA-IASB and KMI-IRM are all contributing to the Network for the Detection of Atmospheric Composition Change (NDACC): relevant results from AGACC will be discussed in this international community, and possibly submitted to its database. The results will also be available to model teams, e.g., in the European ACCENT and the SCOUT-O3 community, to enable them to validate and improve their models and predictions for the future. AGACC results will be published and presented at international symposia in order to maximize their use for atmospheric chemistry and climate

applications and in environmental assessments (e.g., IPCC), in support of policy makers and for enhancing the awareness of the public. A dedicated Web site is available.

3 RESEARCH RESULTS

WP 1000 RETRIEVAL AND ITS CHARACTERIZATION OF TARGET CLIMATE-RELATED GEOPHYSICAL PARAMETERS

WP 1100: Water vapour

WP1110: Exploitation of radiosondes measurements at Ukkel

Since 1990, a rather uniform dataset of radiosonde relative humidity profiles is gathered at Uccle. This dataset can form the basis for a time series analysis of the humidity field in the Upper Troposphere – Lower Stratosphere (UTLS) region.

Unfortunately, the radiosonde humidity sensors suffer from several instrumental or calibration shortcomings, e.g. time lag of the response, inaccurate calibration model for the temperature dependence of the response at low temperatures, solar radiation dry bias, chemical contamination dry bias, icing during the ascent,… In the literature, two different and independent (dry) bias corrections have been suggested by Leiterer et al., 2005 and Miloshevich et al., 2004. After comparison of the humidity profiles corrected by either method with simultaneous data measured by another radiosonde type on the same balloon, we conclude that the Miloshevich method tends to overcorrect the humidity profile in UT conditions (i.e. at low temperatures and high relative humidity). This finding is in agreement with studies based on the comparison of radiosonde data with data from independent and well-calibrated hygrometers (Suortti et al., 2008). We therefore chose to correct our database with the correction method developed by Leiterer et al.

Nevertheless, after correction, a dry bias persists in the humidity profiles, even at the lower tropospheric layers. A supplementary indication for this dry bias is given by the comparison of the total integrated water vapour amount (IWV) calculated from or measured with four different instruments at Uccle: radiosondes, Global Positioning System (GPS), the CIMEL sun photometer, and the Fourier Transform InfraRed (FTIR) spectrometer operated by BIRA-IASB and ULB. Although a very good agreement between these datasets is obtained (see Figure 1), the IWV values calculated from the radiosondes are on average smaller than these measured by the CIMEL and GPS. An overview of the results of the intercomparison of the different techniques is given in Table 1. The source of the differences in the water vapour content measurements will be investigated in more detail in the second phase.

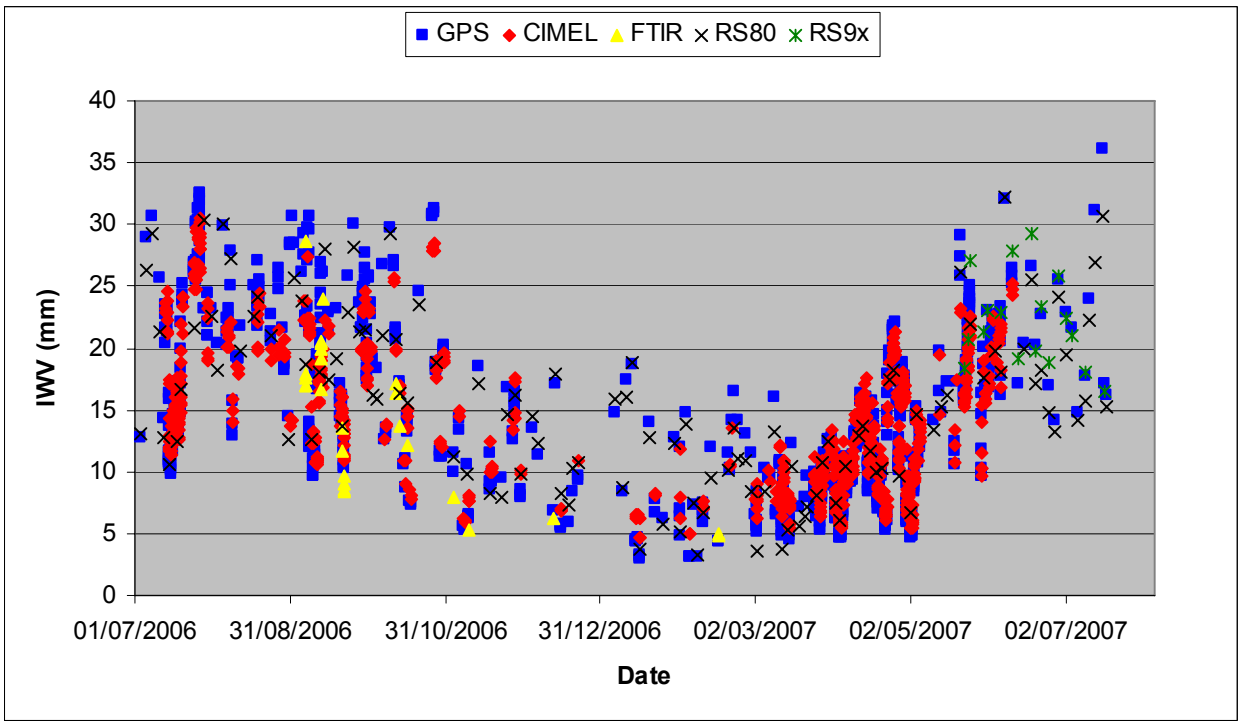

Figure 1 : Comparison of simultaneous integrated water vapour (IWV) amounts at Uccle measured by 4 different techniques (5 instruments) for the period July 2006 to June 2007. The vertical humidity profiles measured by radiosondes were corrected with the Leiterer method (RS80) or the Miloshevich method (RS9x) before calculating the IWVs.

	Bias (mm)	RMS (mm)	N	RMS/$\sqrt{N}$	Comments (1→2)	Slope	Intercept	R^2
CIMEL-GPS	0.04	2.03	795	0.072	No bias	0.81	2.71	0.92
gbFTIR-GPS	-2.64	3.58	25	0.716	Dry bias	0.82	0.25	0.87
RS80-GPS	-1.35	2.23	123	0.199	Dry bias	0.87	0.92	0.96
RS9x-GPS	0.91	1.41	17	0.342	Wet bias	1.01	0.66	0.91
CIMEL-RS80	0.74	1.91	32	0.338	Wet bias	0.91	1.88	0.91
FTIR-CIMEL	-1.37	3.11	16	0.778	Dry bias	1.14	-3.60	0.74
gbFTIR-RS80	-2.4 -2.7	2.7 3.0	11 36	0.814 0.500	Dry bias Dry bias	0.91 0.98	-0.73 -2.44	0.86 0.92

Table 1: Results of different intercomparisons between instruments measuring IWV (in mm) at Uccle. RMS: root-mean-square standard deviation of the differences; N: number of measurements in the comparison data sets; Slope, Intercept and R2 define the correlation line and the correlation coefficient, respectively.

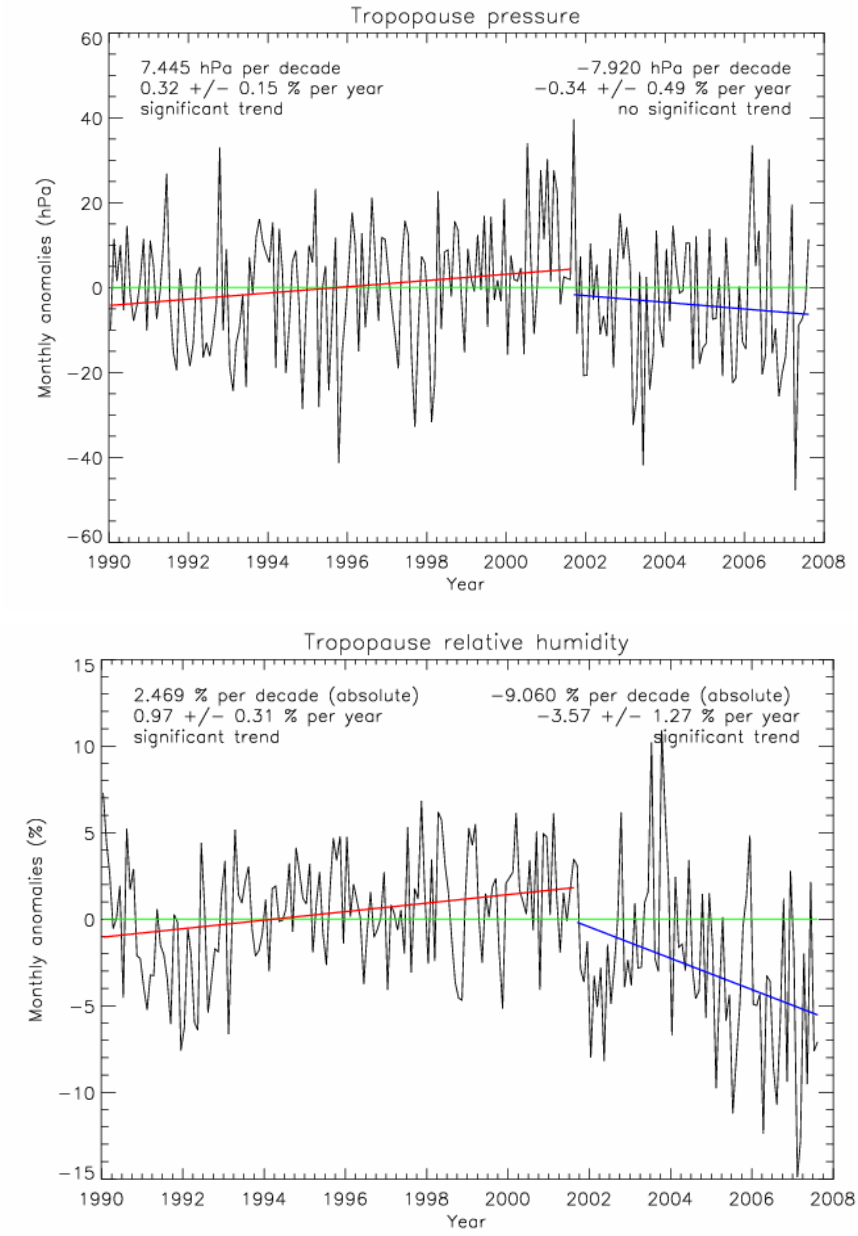

Figure 2: Trend analysis results for the monthly anomalies calculated for the tropopause pressure (in hPa, upper panel) and relative humidity (in %, lower panel). The time series are split up in two parts: one before and one after the September 2001 change points, and trends are calculated for the partial time series.

The 1990-2007 time series of corrected relative humidity profiles was then further used for a trend analysis. In order to cancel out the seasonal variation in the data, we worked with monthly anomalies, i.e. for each month the deviation from the total monthly mean (= the monthly mean taken over all years) is calculated for a given variable. Change points in the time series were detected by applying the Pettitt-Mann-Whitney statistical test. The most important conclusions can be summarized as follows (see figure 2). The UT and tropopause layer were moistening until around September 2001, followed by a strong drying from that date on. This consecutive moistening and drying of the UT and tropopause layers seems to be caused by a lifting, respectively lowering of the tropopause. Indeed, the September 2001 change point was also present in the tropopause pressure and height time series. The origin of this change point is not well understood and needs to be investigated in more detail.

WP1120: Intercomparison campaign - radiosondes and FTIR measurements

The AGACC measurements campaign at Uccle took place between 13 July 2006 and 22 April 2007. During this period, about 900 spectra were recorded in the IR during 37 sunny days, and 20 noon PTU soundings were performed by the KMI-IRM. Much effort has been put on the main isotopologue $H_2{}^{16}O$ for radiosonde intercomparison purposes. The selected microwindows were tested one by one, with varying retrieval parameters. Sixty-two spectra recorded during 12 different days are available for analysis. Among them, 37 were recorded on the same day of a radiosounding, but for only 11 of them recorded on 4 different days the temporal noon coincidence with the sonde was achieved. The coincidence criteria have been set as: ± 75 minutes time difference between sonde launch and FTIR spectrum acquisition. Results are presented as total columns, partial columns and profiles. The FTIR retrieval strategies for H_2O and its isotopologues are identical to the ones reported in the AGACC mid-term evaluation report, except for some minor modifications.

Total columns (expressed as molec/cm^2) have been converted to Total Precipitable Water (TPW) or Integrated Water Vapor (IWV, mm or l/m^2) and comparisons have been made with CIMEL, sondes and GPS data. These results were included in the comparisons presented in WP1110 (Figure 1). A systematic dry bias of FTIR with respect to the sondes data could be seen.

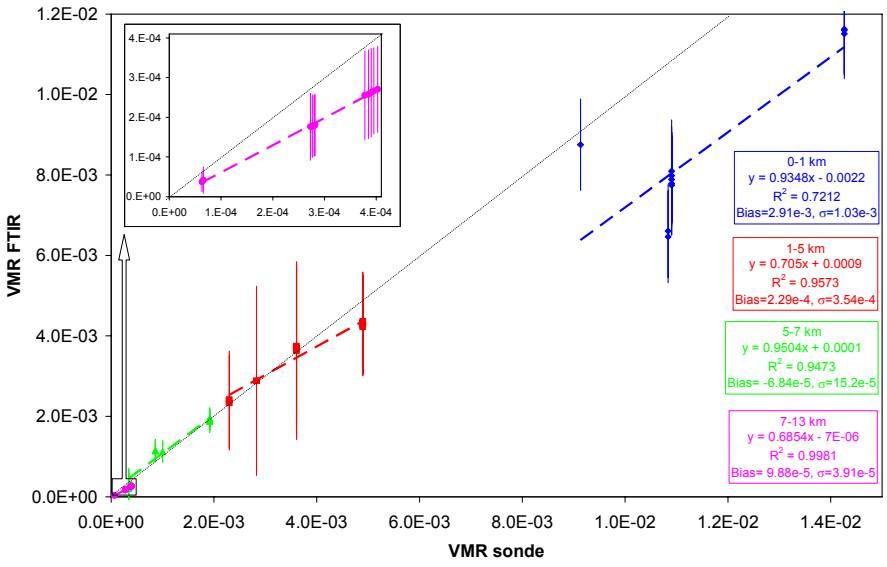

Figure 3: Retrieved $H_2{}^{16}O$ profiles in log[volume mixing ratio] on Sept. 06 2006 and comparison with the coincident sonde profiles. The a priori profile is also shown.

Vertical water vapour **profiles** have been retrieved for the 11 coincident cases and shows good agreement with the sonde measurements from 0 to around 15 km of altitude, which is the maximum altitude of the sonde data. The agreement is especially good on October 11 as shown on Figure 3. Retrievals are able to capture vertical trends in the profiles, although they don't match perfectly with the sondes, especially above 8-10 km where the decrease of the sonde values in 3 out of 4 days is not reproduced by the retrieval. The difference between the FTIR and sonde data, which is obtained by smoothing (i.e. degrade the vertical resolution) of the highly resolved sonde values, is larger between 1 and 3 km.

The characterization of the information comprised in the measurements and error budgets computations have been performed. Typical averaging kernels show that the FTIR observations contain information about the vertical distribution from the surface up to 12 km. The best vertical resolution of the retrieval is observed between 0 and 6 km. The number of

independent layers contained in the retrieved profile is 3 at best. The 11 coinciding pairs show identical results. On the basis of errors and averaging kernels, the sensitivity is max between 0 and 8 km, and the corresponding uncertainty is less than 50%.

The systematic bias for the IWV, observed between FTIR and the sondes, was investigated by comparing well-chosen **partial columns**, i.e. the vertical structures that can be resolved by the FTIR technique (Schneider M. et al., 2008). The following four layers have been defined: 0-1, 1-5, 5-7, 7-13 km.

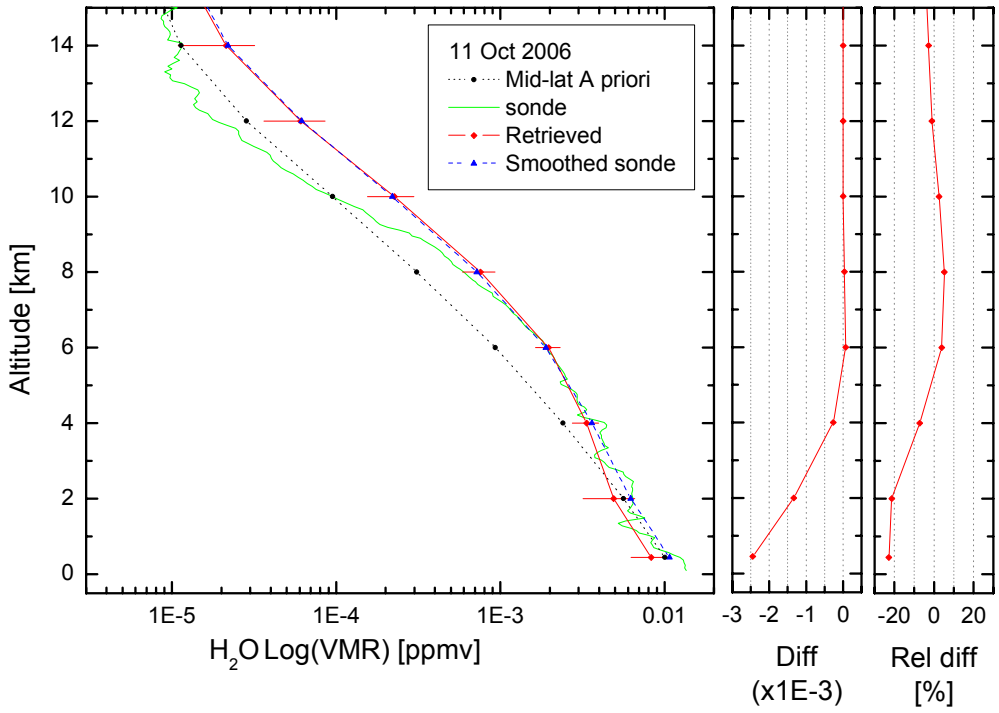

Figure 4: Retrieved $H_2{}^{16}O$ profile in log(vmr) on Oct. 11, 2006 (4 other coincident retrievals gave identical results but are not shown for clarity), and comparison with the coincident sonde profile. The a priori profile is also shown.

Figure 4 shows that the discrepancy mainly comes from the first layer close to the ground, which confirms what was already observed in the vertical profile retrievals and can explain the systematic dry bias for the total columns. While the observed discrepancy is certainly related to the greatest variability of water vapour concentrations in this altitude range, the exact reasons of the systematic bias are not yet well understood, and are under investigation. The agreement is reasonable or even very good for the other layers.

WP1130: Exploitation of FTIR measurements at Ile de La Réunion and Jungfraujoch

The setup of the strategy for water vapour retrievals proposed in this WP has started with the exploitation of spectra recorded at the ***Ile de La Réunion*** in 2004 (in the frame of the ESAC II project). A systematic search for suitable lines was performed over a wide spectral region (Notholt J. et al., 2006; Schneider, M. et al., 2005, Meier, A. et al., 2004, Kuang, Z. et al., 2003) and microwindows for the different isotopologues were then selected. Retrievals of $H_2{}^{16}O$, $H_2{}^{18}O$

and HDO vertical profiles and $H_2{}^{17}O$ total columns from the FTIR spectra were performed using the *Atmosphit* software (Barret et al., 2005; Hurtmans et al., 2005). Extensive investigations were conducted to determine the most suitable retrievals parameters for the different isotopologues. The most important outcomes are briefly summarized below.

For $H_2{}^{16}O$, 4 independent pieces of vertical information vertical distribution, mainly located between the ground and 7 km could be extracted. The retrieved profiles and total columns were compared to coincident sondes measurements and a good agreement was obtained.

For $H_2{}^{18}O$, vertical profiles are obtained for the first time. They also contain 4 independent pieces of information, and possess a vertical sensitivity similar to that of $H_2{}^{16}O$.

For HDO, the coupling of 2 well-chosen micro-windows gave improved results compared to a single micro-window, both in terms of the quantitative information that could be extracted from the measurements and of the error budget. This approach allowed extracting 3 pieces of information with a vertical sensitivity again similar to that of $H_2{}^{16}O$ in the best cases.

Finally, for $H_2{}^{17}O$ only total columns can be retrieved because it is characterized by very weak absorption, and the retrieval of the vertical profiles therefore failed up to now.

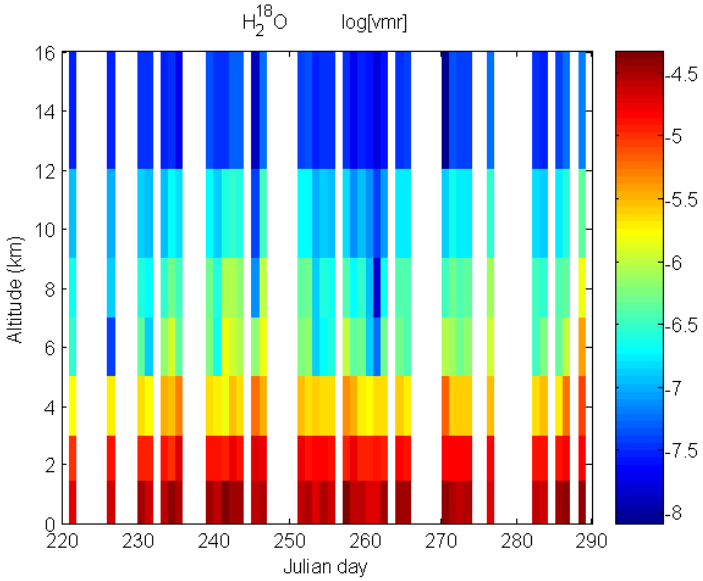

Figure 5: Temporal evolution of the $H_2{}^{18}O$ vertical profiles during the 2004 campaign.

This work allows producing temporal variations over the 2004 campaign duration. Figure 5 shows the temporal trends of the $H_2{}^{18}O$ vertical profiles as an example between 20th Aug. and 24th Oct. 2004. Such results are presented for the first time, and a thorough interpretation is still limited therefore.

The third measurement campaign at ***Ile de La Réunion*** was successfully held between May and October 2007. We focused on the comparisons between the ground-based FTIR and the IASI satellite measurements (Infrared Atmospheric Sounding Interferometer onboard MetOp) (Clerbaux C. et al., 2007), which also provide information on the water isotopologues vertical distributions (Herbin et al., 2007).

One specific day, with a very good time and space collocation (± 3 hours time difference; ±1° latitude and longitude difference), was chosen for this first case study. Typical $H_2{}^{18}O$ and HDO profiles obtained from satellite and ground-based spectra are compared in Figure 6 where the 2 most coincident spectra of each type are shown. The agreement for $H_2{}^{18}O$ is reasonable but for HDO, the vertical profiles show larger differences between 3 and 7 km, although the total columns agree with each other within the error bars for the two species.

A preliminary investigation of isotopic ratios was performed. Depletion of heavier water isotopologues relative to the SMOV (Standard Mean Ocean Value) is measured in parts per thousand using the conventional notation. For HDO, it is defined as:

$\delta D = [(R / R_{SMOV}) - 1] \times 1000$, where R equals $HDO/H_2{}^{16}O$ and R_{SMOV} denotes the isotopologic mass ratio (= $0.31152.10^{-3}$). The δD values obtained from the IASI retrievals are presented in Figure 7. They show depleted values comprised between -700‰ and 0 that are compatible with the theoretical distillation curve up to 10 km. Above 10 km, a positive trend is observed, which could be explained by an uplift of cold air (less dehydrated, less depleted) from the cold point. Despite large variability and error bars (that might be overestimated because correlations between the species are neglected), the obtained values are consistent among a series of spectra and they are also consistent with values reported in the literature (Herbin et al., 2007).

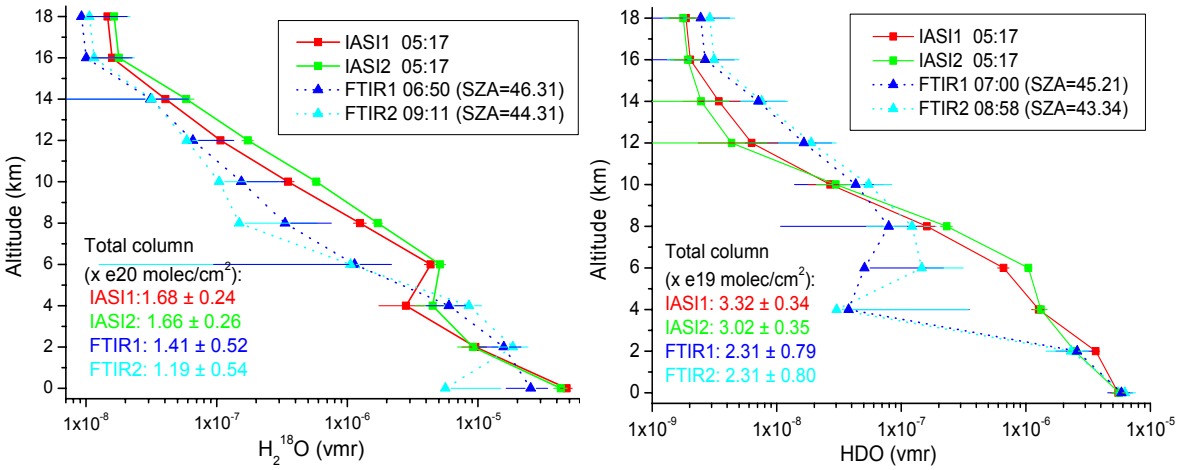

Figure 6: Comparison between vertical profiles (in volume mixing ratio) obtained from the 2 best coincident IASI (red and green squares and lines) and FTIR ground-based spectra (blue and light blue triangles and dotted lines). Left: $H_2{}^{18}O$; Right: HDO.

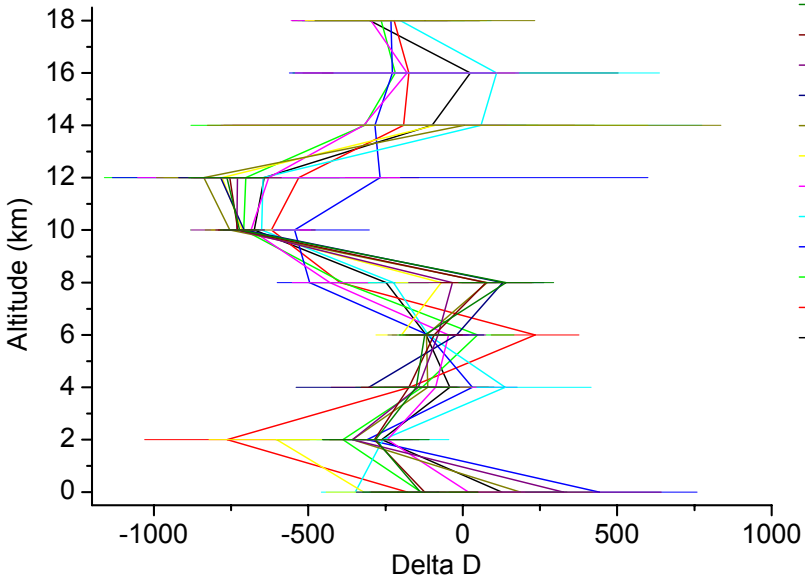

Figure 7: δD profile (in ‰) obtained from the selected 12 IASI spectra recorded above Ile de la Réunion on May 25, 2007.

Preliminary investigations have been performed to derive profiles of water vapour from **Jungfraujoch** infrared solar observations. To retrieve water vapour from the FTIR spectra, more than 60 microwindows, encompassing one or several H_2O lines and located in spectral regions ranging from 700 to 4300 cm^{-1}, have been selected and tested to develop a robust fitting strategy. The contribution of different error sources to the total error was investigated (Figure 8).

Combination of several micro-windows should allow to increase the quantity of information retrieved from the spectra. However, inadequacies in the spectroscopic parameters describing the different lines worsen the quality of the fittings of the spectra when several micro-windows are used. We hope to improve these parameters by collaborating with colleagues analysing H_2O in laboratory, in particular with the department of photophysics at the University of Brussels. Another problem is the inability to accurately reproduce the observed shape of water vapour absorption lines with a Voigt line profile (see for example Boone et al., 2007), which is used in most of the retrieval software.

At this stage, averaging kernels analysis indicates a quite good sensitivity from the altitude site (3.58 km) up to 11 km. We hope to derive 3 to 4 independent pieces of information on the water vertical profile. In the most favourable cases, the sensitivity range may extend up to 15 km.

Investigation of micro-windows containing water vapour isotopologues ($H_2{}^{17}O$, $H_2{}^{18}O$ and HDO) has also started. The analysis of the atmospheric isotopologic water vapour composition provides valuable information on many climate, chemical and atmospheric circulation processes.

Current investigations focus on the vertical grid discretization we use in our model. It seems that we have to use thinner layers, especially in the troposphere, because of the huge vertical gradient of water in this region. Until now, we worked with a 41 layers model. We have developed programs to redefine a-priori volume mixing profiles and pressure-temperature profiles with more layers. We currently test models with up to 100 layers, carefully chosen to avoid abrupt changes in layer width, which lead to oscillations in retrieved profiles.

Future work on the Jungfraujoch observations:

- optimize the retrieval strategy: define the best conditions for the retrieval (find the most appropriate vertical grid, test the analysis in a log-scale with PROFFIT software)
- compare H_2O FTIR retrievals with retrievals from other sources (Payerne soundings, Jungfraujoch photometer and GPS, Bern microwave radiometer, …)

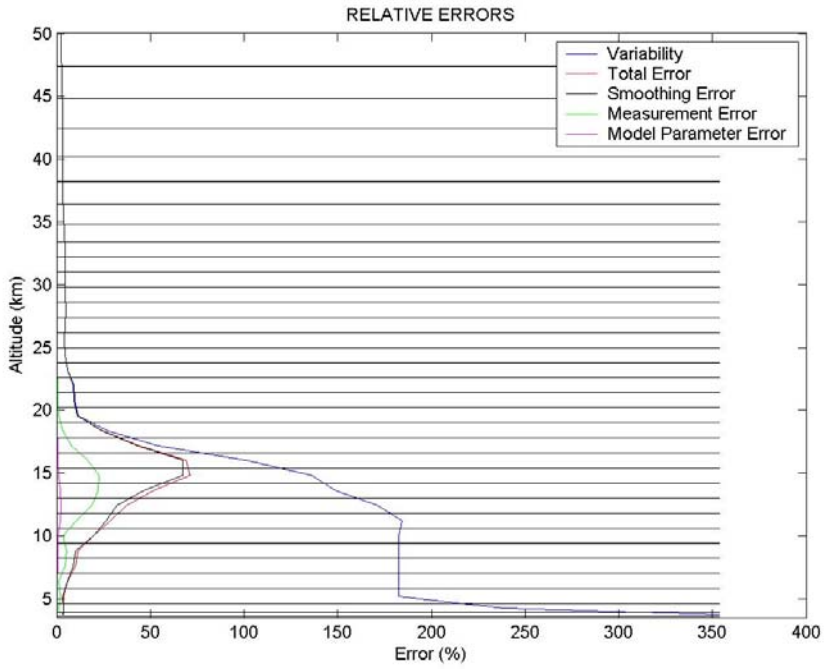

Figure 8: Error budget for the FTIR measurements of water vapour at Jungfraujoch.

WP1200 Aerosol properties

WP1210 CIMEL sunphotometer measurements

The CIMEL instrument was installed at Uccle (50.5°N, 4°E). The sunphotometer operated correctly from July 2006 until September 2007, providing data to the AERONET network (Holben et. al, 1998). During the time period October 2007-Februari 2008 the instrument was recalibrated (standard intercalibration with an AERONET master instrument at Carpentras (44° N, 5° E)). Since March 2008 the recalibrated sunphotometer is fully operational again. The processed data, e.g., aerosol optical depth (AOD), aerosol size distribution, and integrated water vapor (IWV), are available on the AERONET website (http://aeronet.gsfc.nasa.gov/), and have been used in several studies since then.
The data from the CIMEL instrument have been of substantial use for the scientific community in Uccle: S. Dewitte et al., 2007 used the data to perform an analysis of the solar radiation at Uccle from a climate change point of view. The AOD data has been used in an intercomparison of AOD retrieved from the CIMEL measurements and from Brewer ozone measurements by A. Cheymol et al., 2008. The CIMEL was also included in an intercomparison study of IWV measurements from radiosonde, sunphotometer, FTIR, and GPS instruments, as part of WP1100.

WP1220 MAXDOAS measurements

Figure 9: Picture of the MAXDOAS instrument developed at BIRA-IASB

A MAXDOAS instrument optimized for the retrieval of aerosol properties was developed at BIRA-IASB. A picture of the instrument is shown in Figure 9. Initially, the instrument will be operated in Uccle, measuring the O_2-O_2 absorption in spectra of the scattered sunlight that are

recorded in various directions. To retrieve the vertical profile of the aerosol extinction coefficient in the range from 0–3 km altitude and the total AOD, a retrieval algorithm was developed. First tests were performed to validate the algorithm.

1. The MAXDOAS instrument

The newly developed multi-axis differential optical absorption spectroscopy (MAXDOAS) instrument, schematically represented in Figure 10, consists of three main parts: a thermo-regulated box (Figure 10A) containing two spectrometers (Figure 10B and C) located inside the building, the optical head (Figure 10D) mounted on a suntracker (Figure 10E) located outside connected to the spectrometers via optical fibers, and the controlling and acquisition unit (Figure 10F and G). Here we will present a short description of the instrument.
The MAXDOAS instrument developed for AGACC is a full dual-channel system. A two-way splitter fiber optic bundle with rectangular terminations links the output of the optical head with the two spectrometers. The optical head design is such that the telescope (Figure 10D) can be moved in a wide range of elevation (0-90°) as well as azimuth directions (0-360°). In addition the optical head is mounted on a commercial sun tracker from the BRUSAG company (INTRA). This set-up enables not only scattered light, but also direct-sun measurements. The sky radiances are collected by an off-axis parabolic mirror (Figure 10D.2) within a 1° field of view. The optical head also includes a 6-position filter wheel (Figure 10D.3) equipped with transmission diffuser plates, (eventually) linear polarizers and band pass filters.
The optical head collects the direct-sun and scattered light at various elevation and azimuth angles. The light is guided to the two spectrometers through two unique optical fibers. The first spectrometer (Figure 10B), a commercial grating spectrometer from New Port (model MS260i), covers the UV region (300-390 nm). The grating consists of 1200 grooves/mm blazed at 350 nm. The instrument function is close to a Gaussian of full width at half maximum (FWHM) equal to 0.6 nm and there is a good sampling (9 pixels at mid-height for line 346 nm). The output of the spectrometer is connected to a low-noise thermo-electrically cooled (to 233K) CCD detector system (Princeton Instruments, model PIXIX 2KBUV, back illuminated, UV enhanced) with 2048x512 pixels (Figure 10 H). The spectral range covered by the second spectrometer (ORIEL MS127) extends from 400 nm to 720 nm (Figure 10C). The detector (Figure 10I) used (Princeton Instruments, back illuminated) has 1340x100 pixels and is kept at 235K by the Pelletier cooling system. The grating consists of 600 grooves/mm blazed at 400 nm. The instrument function is close to a Gaussian of FWHM equal to 0.9 nm. To cut the second order of the grating a high-pass filter (CVI-Melles Griot with a cut-off at 395 nm) is used. The whole system is mounted inside a thermally regulated (Figure 10J) container to minimize thermal stress on mechanical and optical parts.
The controlling unit consists of two synchronized computers. A first "master" computer controls the sun tracker (i.e., elevation and azimuth angle of the telescope), the filter wheel and the acquisition of spectral data from the spectrometer operating in the UV region. The second "slave" computer does a synchronized acquisition of the spectral data from the spectrometer operating in the VIS region. The data acquisition is fully automated using software developed at BIRA-IASB.

Over the last months substantial progress has been made: the development of the instrument has entered his final phase. It is expected that the instrument will be fully operational within the next few weeks and will start to provide us with MAXDOAS measurements. In addition considerable progress has been made on the development of the retrieval algorithm of aerosol properties from these measurements. In the next section we will give a short outline of the newly developed retrieval algorithm and demonstrate its capability to retrieve aerosol extinction vertical profiles and total aerosol optical depths based on simulated MAXDOAS measurements of O_4 slant column densities and relative changes in intensities. An important improvement of this algorithm compared to previously reported

retrieval algorithms, is the implementation of the radiative transfer code LIDORT (Spurr et. al, 2001; Spurr, 2002). This code allows the development of a much faster algorithm as will be outlined in the next section.

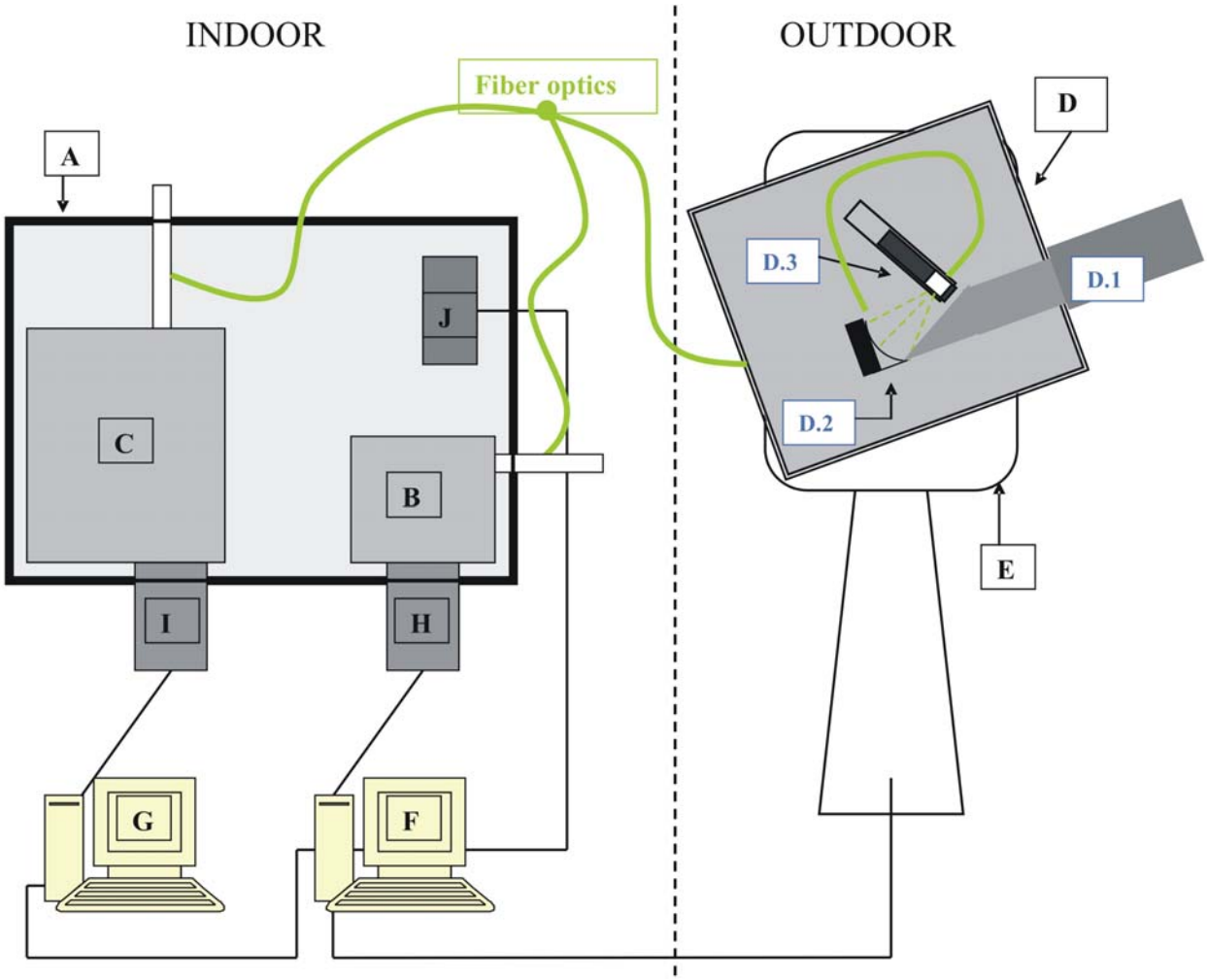

Figure 10: Schematic representation of the MAXDOAS instrument.

2. The measurement and retrieval algorithm

a. General approach

To obtain aerosol properties, including the total aerosol optical depth and aerosol extinction vertical profile, we start from measurements of the differential absorption structures of the oxygen collision complex O_4. Measurements of the slant column densities (SCDs) of a certain absorber for different geometrical configurations (Ω, i.e., the solar zenith angle (SZA), elevation angle and relative azimuth angle) and wavelengths (λ) can provide information on the aerosols when the vertical profile of the absorber is known (Wagner et. al, 2004; Friess et. al, 2006; Wittrock et. al 2004; Irie et. al, 2008). Since the vertical profile of O_4 is well-known and nearly constant (it varies with the square of the O_2 monomer) this absorber is a very good candidate (Greenblatt et. al, 1990). Another advantage of O_4 is that it is mainly concentrated close to the surface. Consequently, the observed O_4 absorption will be very sensitive to changes in the light path distribution due to the presence of aerosols at low altitudes.

The differential SCDs(Ω,λ) (i.e., the SCDs relative to a reference spectrum) of O_4 for the different geometries and wavelengths can be obtained from the measured spectra of scattered sunlight based on the so-called DOAS technique using a linear/nonlinear least-squares spectral fitting method (Platt, 1994). In addition the differential intensities I(Ω,λ) (i.e., the intensity –or the detector signal– relative to the reference spectrum) can be obtained from the measurements.
The remaining step is the retrieval of aerosol properties from differential SCDs of O_4 and intensities relative to a reference spectrum observed at different combinations of Ω and λ. In a first stage we tried to retrieve the total aerosol optical depth and the aerosol extinction vertical profile. To this aim, we used the optimal estimation method (Rodgers, 2000) as inversion method. Herein, the aerosol extinction vertical profile **k** is retrieved given an a priori profile $\mathbf{k_a}$, the measurements **y** (here, a set of O_4 SCDs and intensities relative to a reference spectrum at different combinations of Ω and λ), their respective uncertainty covariance matrices ($\mathbf{S_a}$ and $\mathbf{S}_\varepsilon$), the matrix **K** of the weighting functions, and a forward model operator **F** usually implemented as a numerical model. In case of a non-linear problem the solution of the inverse problem can be determined iteratively:

$$\mathbf{k}_{i+1}=\mathbf{k}_i+(\mathbf{S}_a^{-1}+\mathbf{K}_i^T\,\mathbf{S}_\varepsilon^{-1}\mathbf{K}_i)^{-1}[\mathbf{K}_i^T\,\mathbf{S}_\varepsilon^{-1}(\mathbf{y}-\mathbf{F}(\mathbf{k}_i))-\mathbf{S}_a^{-1}(\mathbf{k}_i-\mathbf{k}_a)]$$

The weighting functions indicate the sensitivity of the measurements to a change in the vertical profile. The forward model **F**, describing the physics of the measurement, used here is the linearized discrete ordinate radiative transfer model (LIDORT) (Spurr et. al, 2001; Spurr, 2002). One major advantage of this radiative transfer code compared to other codes (such as Uvspec/DISORT (Mayer and Kylling, 2005) and SCIATRAN (Rozanov et. al, 2005)) is that it includes an analytical calculation of **K** (Spurr, 2002). In previously reported algorithms the weighting functions needed to be calculated iteratively making it the most time consuming step of the retrieval. Eliminating this step by using analytically calculated weighting functions, results in a much faster and much more flexible retrieval algorithm.
Concerning the characterization of the retrieval it is important to know the sensitivity of the retrieved state to the true state (Rodgers, 2000). The averaging kernels –which are the rows of the averaging kernel matrix **A**– express this relationship. They provide a measure for the vertical resolution of the measurement and the sensitivity of the retrieval to the true state at particular altitudes. The trace of **A** provides a measure of the number of independent pieces of information.

b. A first test of the retrieval algorithm

To investigate the potential of MAXDOAS measurements to retrieve aerosol properties using the retrieval algorithm described before, we started from simulated measurements using LIDORT. These measurements consisted of differential O_4 SCDs and relative intensities observed at 10 different elevation angles including 2, 4, 6, 8, 10, 14, 20, 25, 29, and 89.9°, a SZA of 75° and a relative azimuth angle of 90°. The reference spectrum was observed at a SZA and relative azimuth angle of 30° and 90°, respectively.
To check the sensitivity of the retrieval to the presence of aerosols at different altitudes, three separate retrievals were performed based on simulated measurements for an atmosphere containing strongly enhanced aerosol extinction profiles peaking at three different altitudes.
For the retrievals we used the O_4 differential SCD and relative intensities at 4 different wavelengths, 359.7, 477.0, 577.4, and 629.8 nm, corresponding to the maxima of the O_4 absorption lines in the UV/VIS as illustrated in Figure 11.

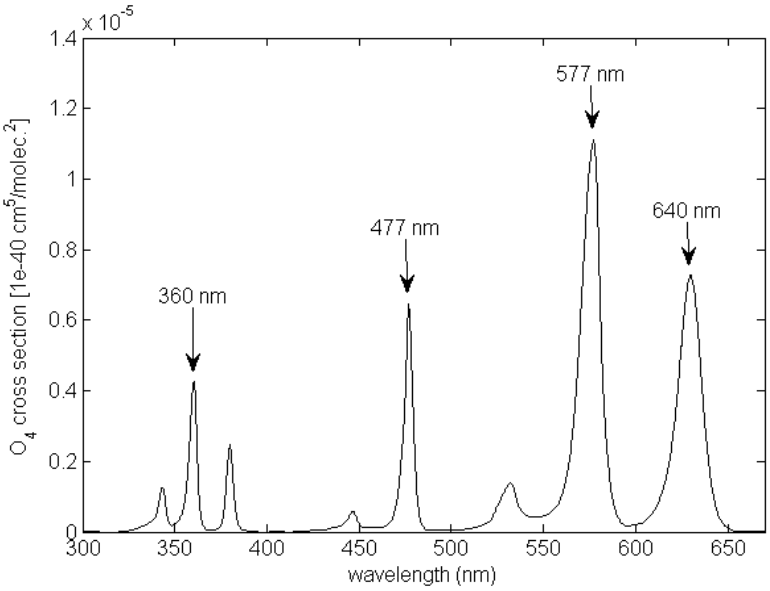

Figure 11: The O_4 cross section, showing the 4 main absorption bands at 360, 477, 577, and 640 nm.

The measurement covariance matrix $\mathbf{S}_\varepsilon$ has been chosen diagonal with values corresponding to 5e-04 times the measurement, assuming that the individual measurement errors are independent. The diagonal values of the a priori covariance matrix were put at 100% of the a priori aerosol extinction at all levels. Non-diagonal terms, introducing a correlation of the aerosol extinction at different altitudes, were added as Gaussian functions as follows: $\mathbf{S_{aij}}=\text{sqrt}(\mathbf{S_{aii}S_{ajj}})\exp(-\text{abs}(z_i-z_j)/\eta)$,
where z_i and z_j are the altitudes of i^{th} and j^{th} levels, respectively and η is the correlation length put at 0.5 km (Barret et. al, 2002). A smooth a priori profile with a total aerosol optical depth (AOD), i.e., vertically integrated extinction profile, of 0.55 was used for the retrievals.

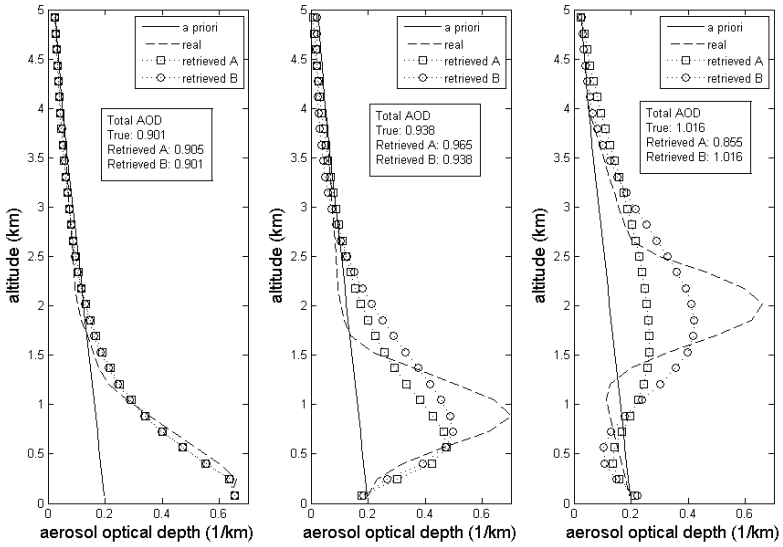

Figure 12: Examples of the aerosol extinction vertical profile retrievals A (only differential SCDs or DSCDs) and B (DSCDs and relative intensities) for a layer of strongly enhanced aerosols (left) at the surface and around (middle) 1 km and (right) 2 km. The solid lines are the a priori profiles, the dashed lines the true profiles, and the circles indicate the retrieved profiles. Also indicated are the total aerosol optical depth of the true profiles and the retrieved total aerosol optical depth.

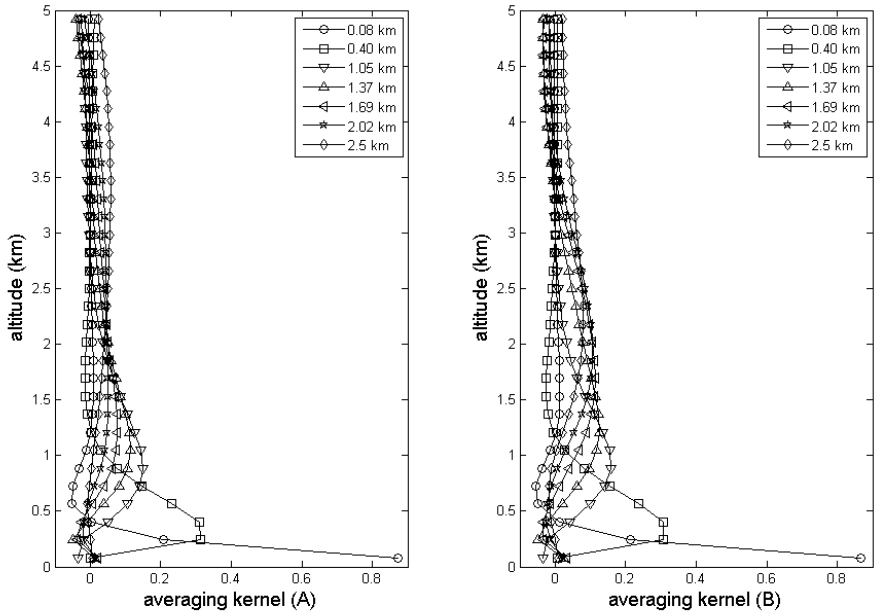

Figure 13: Averaging kernels for the different retrieval altitudes for the aerosol extinction vertical profile retrievals A (left) and B (right) for a layer of strongly enhanced aerosols located at around 2 km.

The results of the aerosol extinction vertical profile retrievals and total AODs are shown in Figure 13 for two different retrieval scenarios. In scenario A only the differential SCD of O_4 were used, while in scenario B measurements of the differential O_4 SCD were combined with relative intensity measurements. It appears that including the relative intensities in the retrieval improves the retrieval of the total AOD. Aerosol extinction profiles located at the surface can be very well retrieved from the MAXDOAS measurements at different elevation angles for both retrieval scenarios. The enhanced aerosols at 1 km and 2 km altitude are also reproduced by the retrieval although the retrieved profiles are smoothed as a result of the limited vertical resolution of the measurements. It appears that adding the relative intensities to the retrievals scenario improves the vertical resolution at higher altitudes.
To get a better estimate of the vertical resolution of the retrievals the averaging kernels for the aerosol extinction profile retrievals A and B for the layer of enhanced aerosols located at around 2 km are shown in Figure 13. The trace of the averaging kernel matrix for these retrievals was ~4. Not much extra information seems to be added by including the relative intensities. The averaging kernels of retrieval B from the surface up to 2 km peak at their nominal altitudes indicating that the retrieval is sensitive for the aerosol extinction profile up to altitude about 2 km. For retrieval A this is only so for the averaging kernels up to ~1.3 km. The vertical resolution of retrieval B, estimated from the full width half maximum of the corresponding averaging kernel, ranges from about 200 m at the surface to about 2 km at 2 km altitude. For retrieval A, the vertical resolution at the surface is similar, but is strongly degraded going to higher altitudes.

3. Future outlook

The MAXDOAS instrument will be finalized and installed at Uccle. Measurements will start in the near future.
To validate the retrieval algorithm it will be applied on real measurements of O_4 differential SCDs and intensities. Obtained AODs will be compared with AODs from the co-located CIMEL instrument.

The retrieval of aerosol properties can potentially be further improved by including additional quantities measured by the MAXDOAS instrument, such as, the magnitude of the Ring effect. Equipping the MAXDOAS instrument with a polarization filter can provide information on the relative contribution of Mie scattering and thus on the atmospheric aerosols. Furthermore, an absolute radiometric calibration of the instrument would further improve the information content of the measurements.

WP 1230 Intercomparison of aerosol measurements

The relative intensities of sunlight from the CIMEL and the Brewer have been compared on clear sky days. The CIMEL filter is centered at 340 nm whereas the Brewer originally operates at 320 nm. To eliminate the difference in ozone absorption at both wavelengths in the comparison of the intensities of both instruments, an adapted observation routine was created for the Brewer instrument, so that it also records the direct sun intensities at 340nm. Additionally, as the Brewer measures with a very narrow bandwidth, the data at several adjacent wavelength steps are filtered to mimic the CIMEL band-pass. With this new observation mode, we get an excellent agreement between the Brewer and CIMEL relative intensities at this wavelength. We are now building up a database of simultaneous intensities of the direct solar irradiance at 340nm in order to compare the AODs derived from both instruments.

We have also compared the AODs retrieved from the Brewer measurements at 320nm with the Langley plot method (Cheymol et al., 2006) with the AODs from CIMEL at 340nm. We have found that the diurnal variation of the AODs calculated from the CIMEL or the Brewer is very similar. Next, all simultaneous clear-sky data ($\Delta t < 3'$) of the CIMEL-Brewer intercomparison campaign were selected, which corresponds to a dataset of 368 measurements, and the AODs were calculated at 320nm and 340nm for the Brewer and CIMEL instruments respectively. We obtain a very good agreement between both instruments (the correlation coefficient being 0.96).

WP 1240: Brewer AOD and UV index prediction

In order to improve the operational UV index prediction at Ukkel, we have investigated the impact of the AOD, measured by the Brewer spectrophotometer #16, on the UV index. Therefore, we implemented the daily/monthly/annual mean of the Brewer AOD at 320 nm in the Madronich TUV index forecast model, instead of using the AOD at 340nm given by the standard Elterman aerosol profile. For 50 clear days, these *simulated* UV indices are compared with the *observed* UV indices, measured by the Brewer instrument. We find that using the daily mean of the observed Brewer AODs improves the UV index forecast significantly and to a larger extent instead of using monthly or annual means. Another important conclusion is that the AOD impact on the UV index increases with the solar zenith angle (SZA) (Cheymol et al., 2007), i.e., a certain increase of AOD reduces the UV index relatively stronger at higher SZA than at lower SZA.

WP 1300: Climate-related trace gases

In addition to water vapor which has been the subject of a previous section, other important direct - and even indirect - greenhouse gases are also targeted by AGACC. The present chapter will report about results acquired thus far for methane isotopologues, HCN, C_2H_2 and formaldehyde (HCHO). Strategies have been developed or tuned in order to retrieve the concentrations of all these species from existing FTIR spectra. In addition, formaldehyde is now also retrieved from UV-Visible MAXDOAS spectra. The complementarity / synergy between both datasets (FTIR and MAXDOAS) will be discussed.

1. Retrieval of formaldehyde profiles and columns using ground-based MAXDOAS and FTIR measurements in April-May 2007 during the AGACC campaign in Ukkel

Formaldehyde (HCHO) profiles and columns have been retrieved for some days in April-May 2007 using ground-based MAXDOAS and FTIR observations performed during the AGACC measurements campaign held in Ukkel. A CIMEL photometer measuring the aerosol optical depth (AOD) and several meteorological instruments were also involved in this campaign. Hereafter, we report on the MAXDOAS and FTIR HCHO retrievals and on the comparison between profiles and columns retrieved using both techniques. Technical details about the retrievaml strategies have been given in the AGACC mid-term evaluation report.

a. Retrieval of HCHO profiles and columns using MAXDOAS observations

Time-series of HCHO DSCDs and maximum air temperature for the April-May 2007 period are presented in Figure 14.

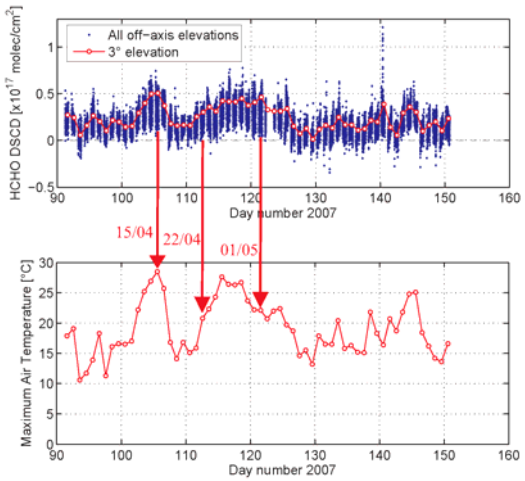

Figure 14: Time series of HCHO DSCDs (upper plot) and maximum air temperature (lower plot; data from KMI-IRM) in Ukkel for the April-May 2007 period. In the upper plot, blue dots correspond to DSCDs at all elevation angles except zenith (reference) and the red dots are the daily averages of HCHO DSCDs at 3° of elevation.

A clear correlation is found between high HCHO DSCDs and high temperature events. A possible explanation for this feature could be that the high temperatures combined to the high surface pressures observed during April-May 2007 in Belgium have favoured the accumulation of formaldehyde precursors (mainly hydrocarbons) and their confinement near the surface as well as their transformation into formaldehyde. This assumption and the correlation of HCHO columns with other meteorological parameters like turbulent diffusion, dew temperature, or downward solar radiation will be investigated in the near future using a tropospheric box model (J.-F. Müller and T. Stavrakou, IASB-BIRA).

Retrieved HCHO profiles and columns are shown and discussed in the subsection on the comparison between FTIR and MAXDOAS profiles.

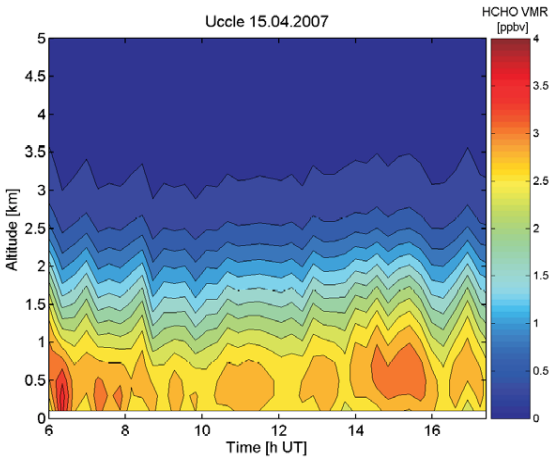

Figure 15: Contour plots of the HCHO profiles (in VMR) retrieved on 15/04/2007.

However, as an example, the contour plot of HCHO profiles retrieved on 15/04/2007 using all MAXDOAS scans below 85° SZA is presented in Figure 15.

b. Retrieval of HCHO profiles and columns using FTIR observations

We focused our analysis on five days during which the meteorological conditions allowed several successive measurements with the same instrumental setup. These days are the 15th, 16th, 21st and 22nd of April and the 1st of May for which 25, 17, 12, 18 and 10 spectra are recorded, respectively.
The obtained degree of freedom on the retrieved HCHO profile lies between 1.2 and 1.7, and the estimated error on the HCHO total column is about 20%.

c. Comparison between MAXDOAS and FTIR profiles and columns

Figure 16 shows the comparison between HCHO total column amounts calculated from MAXDOAS and FTIR profiles for the three selected clear-sky days (April 15 and 22, and May 1, 2007).

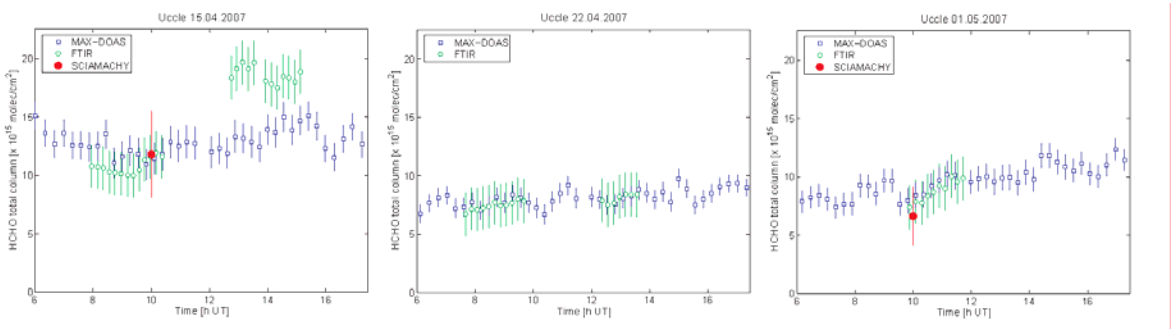

Figure 16: Comparison between MAXDOAS and FTIR HCHO total columns in Ukkel on 15/04/2007 (left plot), 22/04/2007 (middle plot), and 01/05/2007 (right plot). When data exist, the SCIAMACHY nadir column amount corresponding to the daily average of all pixels falling within a radius of 500 km around Ukkel also appears in the plots.

On 22/04/2007 and 01/05/2007, a very good agreement is found between both techniques with relative differences generally smaller than 9 % and never larger than 13 %. We see also that MAXDOAS and FTIR total columns display almost identical short-term variations. On 15/04/2007, larger discrepancies are obtained, especially in the afternoon where FTIR gives

significantly larger column values (up to +38 %) than MAXDOAS. Different sensitivity tests have shown that the FTIR retrieval settings and the impact on the MAXDOAS retrieval of the assumption made on the aerosol loading cannot explain this feature. Since in the afternoon, the MAXDOAS and FTIR instruments are pointing in opposite direction (NE for MAXDOAS and SW for FTIR), we cannot exclude that both instruments probe air masses with very different HCHO content: due to the presence of a large forest area in the South of Ukkel and the high air temperature observed on 15/04/2007 (see Figure 14), large biogenic emissions of HCHO could occur, and with favourable wind direction and speed, would only be detected by the FTIR instrument. We will investigate on this scenario in the near future using tropospheric modelling studies. Concerning the comparison with SCIAMACHY, a very good agreement is obtained on both 15/04/2007 and 01/05/2007.

It is also interesting to note that the FTIR data also show a strong correlation between HCHO total column and precipitable water.

Figure 17 shows examples of comparison results between coincident (time difference smaller than five minutes) FTIR and MAXDOAS profiles on 15/04/2007 and 22/04/2007.

As expected from the total column comparisons, a very good agreement is found between FTIR and MAXDOAS HCHO profiles on 22/04/2007. On 15/04/2007, the afternoon example shows that the FTIR profile is significantly higher than the MAXDOAS one on the whole 0-5 km altitude range. Concerning the morning comparison, the opposite feature is obtained in the 0-2 km altitude range with MAXDOAS profile higher than FTIR. Above 2 km, a good agreement is found between both profiles. The comparison between profiles retrieved on 15/04 and 22/04/2007 also shows that significantly larger HCHO concentrations are obtained on 15/04/2007 up to 3 km altitude and not only in atmospheric layers close to the ground.
The information content has been also characterized through the calculation of the averaging kernel matrices A for both MAXDOAS and FTIR retrievals. Typical examples of averaging kernels are presented in Figure 18.

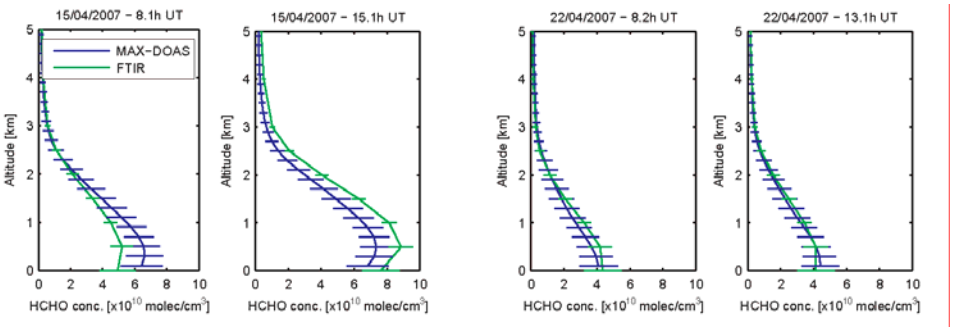

Figure 17: Comparison between coincident MAXDOAS and FTIR HCHO profiles in Ukkel on 15/04/2007 (left) and 22/04/2007(right). The error bars on the profiles correspond to the total retrieval errors.

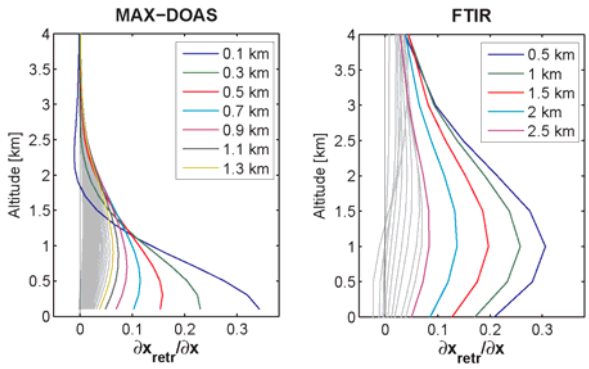

Figure 18: Averaging kernels obtained from MAXDOAS (left) and FTIR (right) HCHO retrievals in Ukkel on 15/04/2007 using measurements around 9:40h UT.

Most of the information on the vertical distribution of HCHO contained in the MAXDOAS and FTIR measurements is located below 1.5 km and 2.5 km of altitude, respectively. These plots also show that both techniques present some complementarity regarding the altitude range where they have their maximum of sensitivity to HCHO: mainly below 0.5 km for MAXDOAS and between 0.5 and 1.5 km for FTIR. Concerning the number of degrees of freedom for signal (trace of A), which represents the number of independent pieces of information contained in the measurements; it ranges from 1.2 to 1.7 for FTIR and from 1.2 to 1.5 for MAXDOAS.

2. Specific setup and approach to retrieve HCHO from the high-altitude site of the Jungfraujoch

At the Jungfraujoch high-altitude site, even the most favorable IR absorptions of H_2CO are very weak. Up to now, reliable HCHO retrievals were only possible using averaged spectra, thus preventing proper characterization of its variability and the production of data for validation. Specific efforts have been undertaken to improve the signal-to-noise ratio (S/N) of the solar observations, with the hope to be able to retrieve H_2CO total columns from individual spectra, with good precision. An experimental setup based on a tunable optical filter covering here the 2810 to 2850 cm^{-1} spectral range has been tested. The combination of a narrower interval with a larger aperture has allowed improving the S/N by more than a factor 4, with the resolution unchanged.

The specific experimental setup has been regularly used since December 2005, allowing to record more than 800 atmospheric spectra. Retrievals have been performed using SFIT-2 (v3.91), HITRAN-2004, a microwindow extending from 2833.07 to 2833.35 cm^{-1} and encompassing a single H_2CO line at 2833.19 cm^{-1}. Interferences by HDO, CH_4 and ozone have to be accounted for. H_2CO total columns have been retrieved for the December 2005 to February 2008 time period (see Figure 19). These first results indicate that: (i) minimum values of about $3x10^{14}$ molec./cm^2 are found in February-March; (ii) higher columns ranging up to $1x10^{15}$ molec./cm^2 are observed during summer; (iii) summer is characterized by higher variability; (iv) a pollution event was detected on 27 July 2006, with H_2CO column about 10 times higher than expected.

The precision achieved on a single measurement has been estimated from inter-spectra variability, to about 10%.

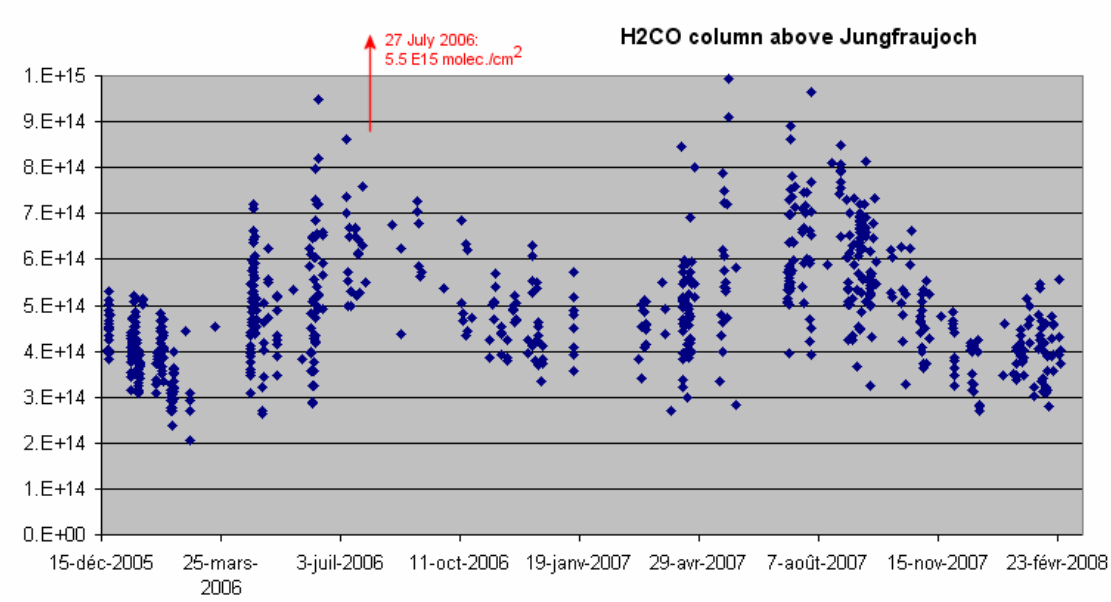

Figure 19: Timeseries of formaldehyde total columns above the Jungfraujoch station.

3. Formaldehyde at Ile de La Réunion

a. *Introduction*

Three measurement campaigns have been performed at Saint-Denis at the Ile de La Réunion in order to prepare for future quasi-continuous observations at the NDACC station at Maido planned from 2010 onwards. During one of the three campaigns (August-October 2004), H_2CO has been measured both by Fourier Transform InfraRed (FTIR) and Multi-Axis Differential Absorption Spectroscopy (MAXDOAS) techniques. As the measurement of H_2CO is a challenge, it is very interesting to compare the results obtained by two independent measurements. The FTIR ground-based total column data of H_2CO are also compared to satellite products retrieved at BIRA-IASB from GOME/ERS-2 (2002) and SCIAMACHY/ENVISAT (2004).

b. *Experimental setup and spectral data analysis*

The FTIR spectra have been recorded using a 120M Bruker Fourier Transform Spectrometer, during three campaigns: October 2002, August to October 2004, and May-October 2007. In 2007, the system was operated using BARCOS (Neefs et al., 2007) that allows the spectrometer to run automatically and to be remotely controlled from Brussels. The retrieval algorithm is SFIT2 (Pougatchev and Rinsland, 1995), which is based on a semi-empirical implementation of the Optimal Estimation Method (OEM) of Rodgers (2000). Vertical profile information can be obtained thanks to the pressure dependence of the absorption line shapes.

Micro-windows (cm^{-1})	Interfering species
2778.20 - 2778.60	CH4, O3, N2O, CO2, HDO
2780.65 – 2781.20	CH4, O3, N2O, CO2, HDO
2855.70 – 2856.50	CH4, O3, HDO
2912.00 – 2912.30	H2O, OCS

Table 2: Micro-windows and interfering species used for the FTIR formaldehyde retrievals.

Four spectral micro-windows are used: they are summarized in Table 2, together with the interfering species.
MAXDOAS measurements have been made in the period August 2004 – July 2005, at the following elevation angles: 0, 3, 6, 10, 18, and 90° (zenith). The spectral range used for formaldehyde is 336-358 nm. The retrievals are made using the WinDOAS software (Van Roozendael et al., 1999). It is also based on the OEM of Rodgers (2000); the profile information can be derived thanks to the dependence of mean scattering height on solar zenith angle and viewing elevation angle.
WinDOAS has also been used to retrieve tropospheric H_2CO columns on a global scale over the period 1997 to 2006, from GOME and SCIAMACHY (De Smedt et al., 2008).

c. *FTIR and MAXDOAS comparisons results: diurnal variability*

The signal of H_2CO in the FTIR spectra is very weak. Since the degrees of freedom for signal (DOFS) is about 1.2, we consider only total columns results. For both the FTIR and MAXDOAS techniques, the vertical information is mainly located below 3 km, where the volume mixing ratio of H_2CO is maximal. As can be seen in Figure 20 for four example days in 2004, the diurnal variability is generally well captured by both techniques and the total columns agree well within their uncertainties. The mean and standard deviation of the

relative differences between FTIR and MAXDOAS results (2*(FTIR-MAXDOAS)/(FTIR+MAXDOAS)) for 25 coincidences are -8 ± 25%.

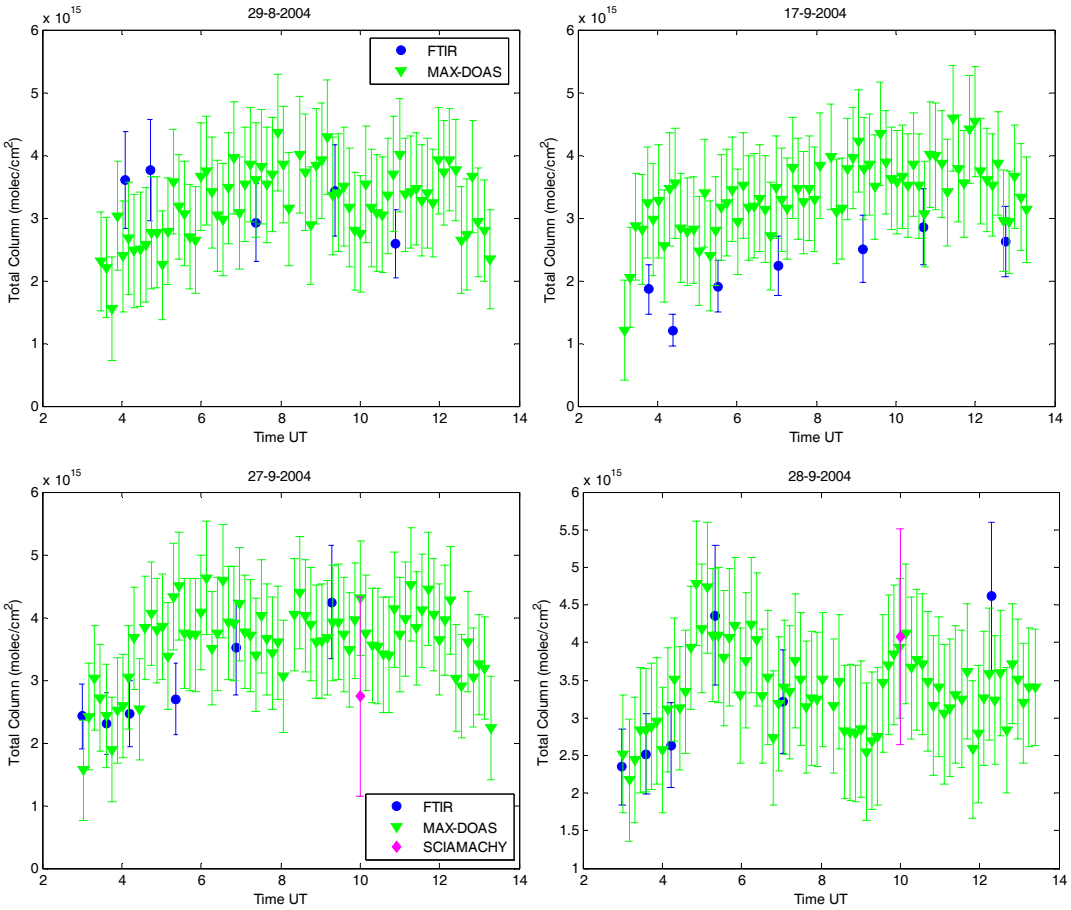

Figure 20: Formaldehyde total columns retrieved from FTIR, MAXDOAS and SCIAMACHY measurements, on August 29, September 17, 27 and 28, 2004 (left-to-right, top-to-bottom).

d. *Comparisons with GOME and SCIAMACHY: daily variability*

We compare daily means of formaldehyde total columns retrieved from FTIR and MAXDOAS spectra and from GOME (2002) and SCIAMACHY (2004) within 500 km around Saint-Denis (Figure 21). The day to day variability is well captured in all cases. We have only 5 coincidences with GOME, but 17 with SCIAMACHY. For the latter, we obtain as mean and standard deviation of the relative differences between FTIR and SCIAMACHY, 2*(FTIR-SCIAMACHY)/(FTIR + SCIAMACHY)= -13 ± 27 %.

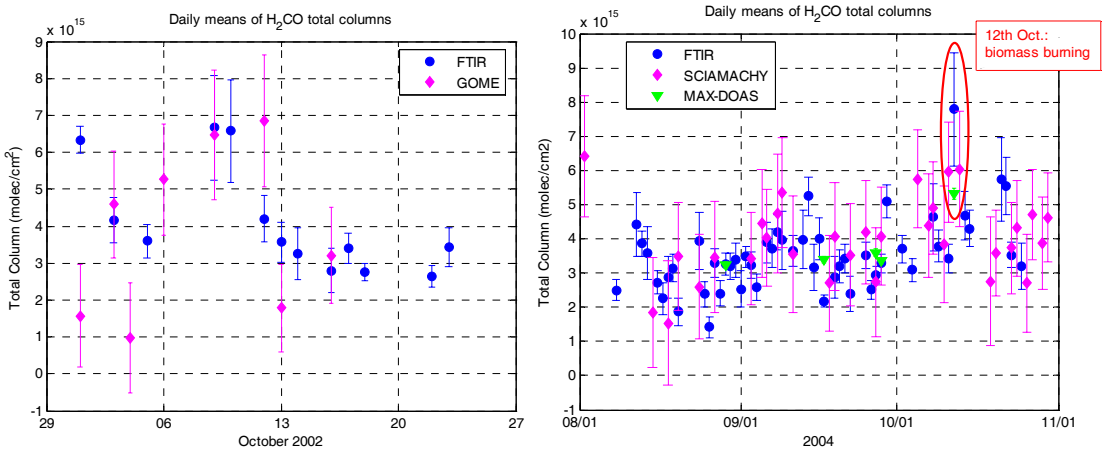

Figure 21: Daily means of formaldehyde total columns. Left-hand plot: 2002 FTIR and GOME data. Right-hand plot: 2004 FTIR and SCIAMACHY data. MAXDOAS data for the four days given in the previous section, and on October 12, are included.

Figure 21(b) shows an enhancement of the formaldehyde total columns on October 12, 2004. It is seen by all 3 instruments, and coincides with enhanced total columns of CO: this event has been attributed to biomass burning in Madagascar and South Africa (Senten et al., 2007).

e. *Seasonality of formaldehyde*

The five months of the 2007 campaign show that formaldehyde has a strong seasonal variation, with a minimum in local winter (August) - see Figure 22.

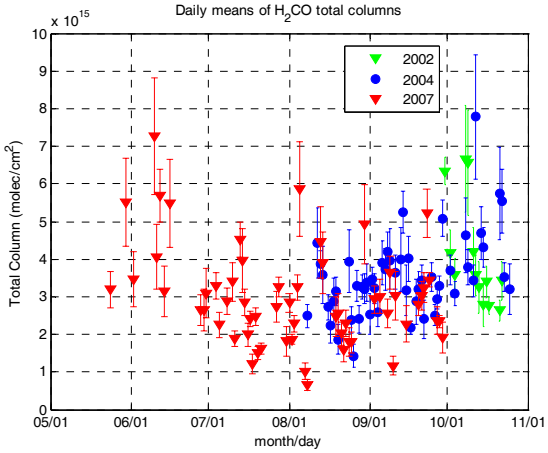

Figure 22: Daily means of formaldehyde total columns retrieved from FTIR measurements during the three campaigns at St-Denis.

f. *Preliminary conclusions*

The results on formaldehyde are very promising. We find a good agreement between FTIR, MAXDOAS and SCIAMACHY total columns. The negative bias found in the comparisons may be due to the use of different spectroscopic parameters (Rothman et al, 2005 for FTIR; Cantrell et al., 1990 for satellite; and Meller and Moortgat, 2000 for MAXDOAS). Comparisons with IMAGES model studies (T. Stavrakou and J.F. Müller) are in progress. A publication is in preparation.

4. Hydrogen cyanide (HCN)

Recent investigations have resulted in the revision of the HCN lifetime from 2.5 years to 2-5 months, more in line with its important and well documented variability in the troposphere. The main HCN source is believed to be biomass burning, making this species a useful tracer of fires. Oxidation by the OH radical is among the identified sinks, while uptake by oceans has been hypothesized as the dominant removal process.

In the 3260-3310 cm^{-1} spectral region, there are several HCN lines that could possibly be used for its retrieval. A systematic and careful look at ***Jungfraujoch*** "dry and wet spectra" has allowed identifying 6 candidate lines close to 3268, 3277, 3287, 3299, 3302 and 3305 cm^{-1}. The major interferences are water vapour, two of its isotopologues ($H_2{}^{18}O$ and $H_2{}^{17}O$) and C_2H_2. Each of the identified lines has been characterized in terms of information content; using a representative subset of spectra, a mean DOFS of 1.6 was computed for the 3287 line, values close to 1.1 were found for the 3268, 3277, 3299 and 3305 lines while the 3302 interval provides less information, with a mean DOFS of 0.75. This latter line was therefore omitted in following tests.

A strategy using simultaneously five HCN lines has therefore been developed, tuned and validated. This retrieval approach has been applied to available Jungfraujoch observations from 1994 onwards. Resulting time series for daily mean partial tropospheric columns are displayed in Figure 23 (left frame).

Among striking features, we notice the very high columns observed in 1998 (and to a lesser extent in 2003) correlated with documented high values of carbon monoxide resulting from important biomass burning; also obvious is the strong seasonal variation with maximum columns generally observed in July. For years corresponding to background conditions (e.g. 2000-2001), the peak-to-peak amplitude amounts to 80% of the mean tropospheric column.

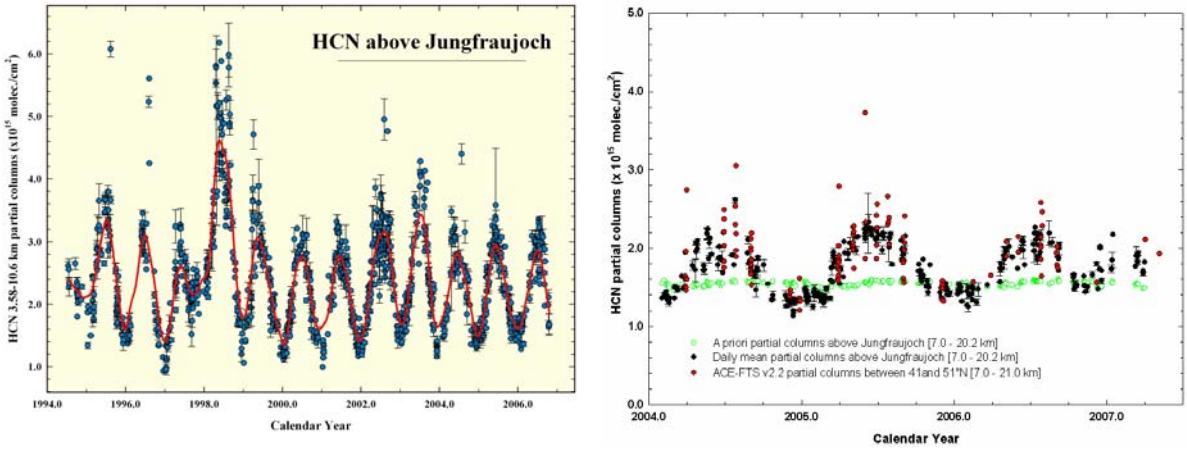

Figure 23: Daily mean tropospheric columns of HCN above the Jungfraujoch station from 1994 onwards (left frame) and comparison with ACE-FTS zonal partial columns (7-21 km) (right frame).

Our retrievals provide good sensitivity up to 20 km, allowing to perform comparisons with ACE-FTS measurements. 117 occultations recorded between 03/2004 and 05/2007 in the 41-51ºN latitudinal belt provide information on the HCN distribution down to 7 km. 7-21 km ACE partial columns have therefore been computed for comparison with the corresponding ISSJ time series. Results are respectively reproduced as black and red circles in the right frame of Figure 23 (while ISSJ a priori partial columns are reproduced in green). These two data sets are in excellent agreement in terms of absolute value, amplitude and phase of the seasonal modulation. An independent check has also been performed, using Jungfraujoch spectra of

2006-2007 and making no use of ACE inputs. This verification has further confirmed the excellent agreement noted above.
The analysis of HCN in spectra from the 2002 and 2004 campaigns at ***Ile de La Réunion,*** using the above strategy was not successful yet, due to even stronger interferences by water vapour. Additional investigations will be made in phase 2 of the project.

5. Methane isotopologues

a. $^{13}CH_4$

Methane is released in the atmosphere by natural processes (e.g. wetlands, termites) as well as by anthropogenic activities (e.g. fossil fuel exploitation, rice agriculture, biomass burning, etc). Due to its high warming potential and its relatively long chemical lifetime (~9 years), atmospheric methane plays a major role in the radiative forcing responsible of the greenhouse effect. Methane also affects climate by influencing tropospheric ozone and stratospheric water. The cycle of methane is complex and to understand it goes through a complete study of its emissions and its budget of sources and sinks, as well as for its main isotopologues.

To study the vertical abundance of $^{13}CH_4$ from high resolution FTIR spectra recorded at the Jungfraujoch, we have selected several $^{13}CH_4$ lines distributed into two sets of microwindows. The first set includes four microwindows in the InSb range, which are fitted simultaneously during the retrievals. The second set contains only one microwindow, in the MCT range.

Figure 24 compares $^{13}CH_4$ partial columns between 3.58 and 14 km, derived from both spectral ranges for the period January 2005- August 2006. A priori partial columns have also been added to point out the good sensitivity of both ensembles. The lower right insert panel also gives the relative mean difference, over the whole time period studied, between experimental points retrieved from each spectral range and the a priori values. The top panel relative differences corresponding to [(MCT-InSb)/InSb]*100 reveal a significant mean bias close to 4% between the two $^{13}CH_4$ partial columns time series. The same mean significant deviation has been observed for the retrieved profiles between 5 and 14 km, indicating that the retrieval strategy doesn't redistribute the $^{13}CH_4$ content above 14 km. However, despite these differences between retrieved values resulting from InSb and MCT ranges, we recommend the use of the MCT microwindow for $^{13}CH_4$ retrievals: the single $^{13}CH_4$ line selected in the MCT range indeed offers a higher information content, a denser set of measurements (due to a wider SZA range for the retrievals) and smaller perturbations by interfering gases (like H_2O and HDO in the InSb set of microwindows).

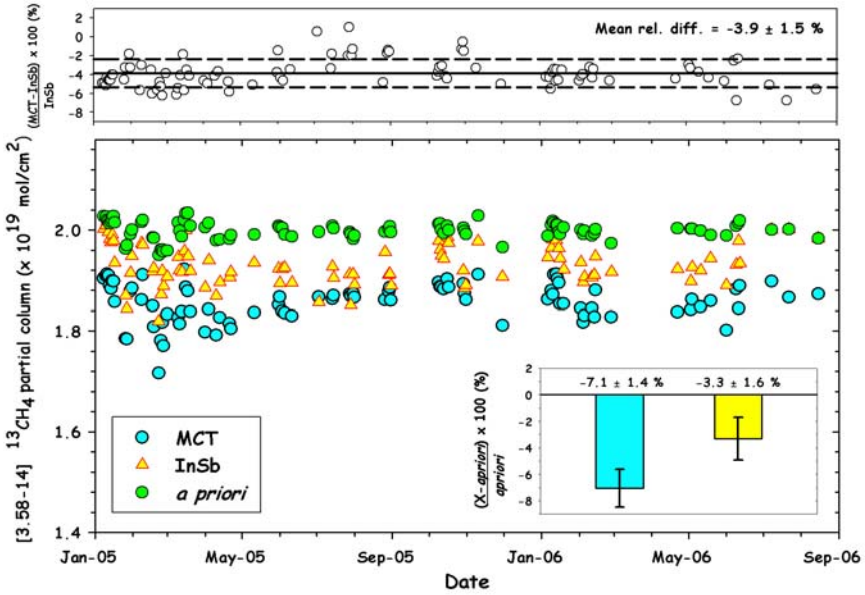

Figure 24: $^{13}CH_4$ partial columns between 3.58 and 14 km derived from MCT line (light blue dots) and InSb lines (yellow triangles). *A priori* partial columns are plotted in green. Lower right insert panel: mean relative differences between each retrieved time series and *a priori* values. Top panel: relative differences between both retrieved time series.

b. CH_3D at Jungfraujoch

Retrievals of CH_3D are more difficult. Four microwindows were identified early in AGACC, but unfortunately 3 of them are polluted by interfering absorptions due to water vapour or HDO. Hence they may not be usable at low altitude and latitude FTIR ground-based stations.

It was therefore important to check if the use of the sole microwindow not affected by water vapour could provide enough information. We have therefore compared the information content related to three different fitting procedures: (i) the use of this microwindow in a single spectrum fitting procedure; (ii) its use in a multi-spectra fitting procedure; (iii) the simultaneous use of the four microwindows in a single spectrum fitting procedure. The multi-spectra approach consists of combining several FTIR spectra recorded during the same day and at the same spectral resolution to increase the information content.

Figure 25 plots daily means CH_3D total columns above Jungfraujoch for the year 2005 and derived from the multi-spectra (yellow triangles) and multi-microwindows (light blue dots) retrieval strategies. Relative differences between the two approaches are plotted in the upper panel. A slight significant relative difference of 1.5 ± 1.0 % can be observed, with the multi-microwindows approach giving higher abundances. A priori CH_3D total columns have also been added (green dots) to emphasize the quite good sensibility of each retrieval strategy. Low insert panel plots relative differences between each time series and a priori values.

It's presently difficult to conclude which approach should be adopted. Even if the multi-microwindows strategy provides higher information content, we don't know at this stage of our investigations if it is applicable to lower altitude sites, much more affected by interferences due to water vapour.

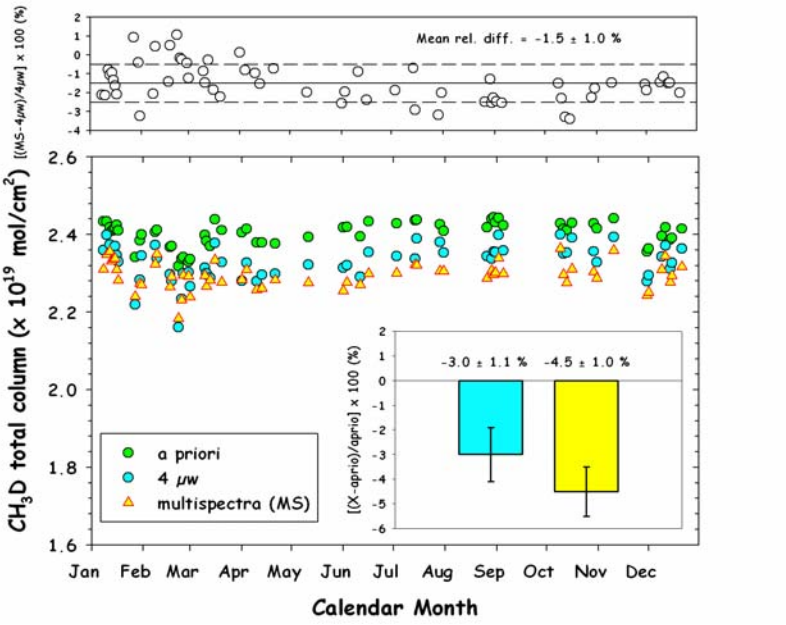

Figure 25: CH_3D total columns derived from the multi-microwindows (light blue dots) and the multispectra (yellow triangles) approaches for the year 2005. *A priori* total columns are plotted in green. Lower right insert panel: mean relative differences between each retrieved time series and *a priori* values. Top panel: relative differences between both retrieved time series.

c. CH_3D at Ile de La Réunion

The retrievals of CH_3D at Ile de la Reunion have been made following the same strategy as performed at the Jungfraujoch (47°N, 8°E) site, and as outlined in the 2006 AGACC report. Given that a large fraction of the CH_3D lines is polluted by many strong H_2O and HDO absorptions, of the 4 spectral regions chosen, 3 still contain significant signatures of H_2O. Due to La Reunion's location, the retrievals are far more sensible to these interferences as compared to a relatively dry high mountain site such as the Jungfraujoch.
However a simultaneous multi-microwindows fitting procedure still yields a much higher information content than an individual microwindow fitting procedure, taking the 3070.71-3071.00 fitting window only.
Note also that only spectra with a solar zenith angle between 70 and 80° have been processed. Lower SZA angle spectra have insufficient information content (DOFS<<1 for the multi-window fit)

Range(cm^{-1})	Interfering species	Line #	DOFS
3070.71-3071.00	CH_4,O_3	2	0.62
All = as above +:			1.06
2950.77-2951.00	HDO,H_2O,O_3	1	
3072.70-3073.15	CH_4,H_2O,O_3,solar lines	1	
3089.15-3089.70	CH_4, H_2O,O_3	2	

Table 3: Selection of microwindows used in the retrieval of CH_3 D, the interfering species and number of CH_3 D lines within each microwindow and, in the last column, the Degrees of Freedom for the single and multiwindow approach.

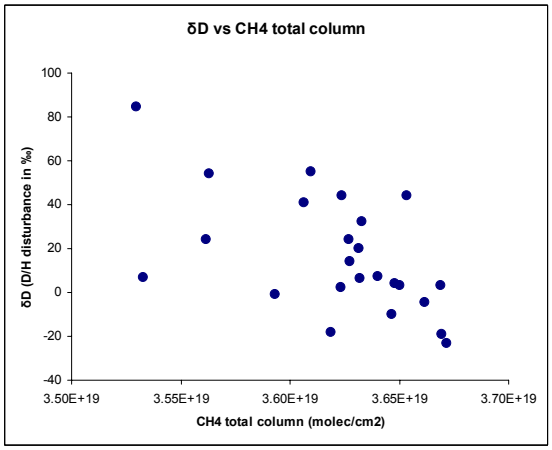

When looking at the retrieved δD, defined as: $\delta D(‰) = 1000 \times [(CH_3D/CH_4)_{sample} / (CH_3D/CH_4)_{standard} - 1]$, where $(CH_3D/CH_4)_{standard} = 155.76 \times 10^{-6}$, we see that δD is indeed higher in old depleted air masses. This is because OH (and Cl) reacts slightly slower with CH_3D than with CH_4 (thus CH_3D has a slightly larger lifetime). The observation of this well established relationship gives confidence to the validity of our retrieval method although further tests still have to be performed.

Figure 26: δD(‰) as a function of total column CH_4

We will further investigate whether we gain information using the multi-spectra retrieval strategy designed at the Jungfraujoch and discussed above.

6. Acetylene (C_2H_2)

Acetylene is among the nonmethane hydrocarbons (NMHCs) accessible to the infrared remote sensing technique. As a product of combustion and biomass burning, it is emitted at the Earth surface and further transported and mixed into the troposphere. Destruction by OH is the main removal process, the resulting average tropospheric lifetime is estimated at 1 month on the global scale. At mid-latitudes, it varies between 20 days in summer to 160 days in winter. This compound is appropriate to study tropospheric pollution and transport, and is often used in conjunction with other tracers of fires.

There are exploitable C_2H_2 absorption lines in both the MCT and InSb spectral domains, more precisely in the 750-780 and 3250-3305 cm^{-1} ranges. Although all these lines are weak (~1% absorption), they can be used for the retrieval of C_2H_2 from ground-based high-resolution IR spectra. A systematic and careful look at ISSJ "dry and wet observations" has allowed to identify 5 candidate lines close to 3251, 3255, 3268, 3278 and 3305 cm^{-1}. The major interferences are water vapor (H_2O) and one of its less abundant isotopologues ($H_2{}^{18}O$). Absorptions by solar spectrum, O_3 and HCN have also to be accounted for. Each of the identified lines has been characterized in terms of information content using a representative subset of spectra. Mean values for the degree of freedom for signal (DOFS) range from 1.2 to 1.5. The final strategy is however reduced to four lines, owing to the fact that the fits to the 3268 cm^{-1} line are less satisfactory.

Information content and error budget have been carefully evaluated. They objectively indicate that our strategy allows to retrieve C_2H_2 tropospheric columns without contribution of the a priori; discrimination between partial columns below and above 7 km is at 92% coming from the retrieval. Typical errors amount to 4% of the tropospheric column, and to 12% of the 7-14.2 km partial columns.

Left frame of Figure 27 shows the Jungfraujoch tropospheric time series retrieved with this new approach (left frame). Among striking features, we notice high tropospheric columns observed in 1998 correlated with documented high values of carbon monoxide resulting from important biomass burning. This is also consistent with record-high troposheric columns of C_2H_6 and HCN observed the same year at the Jungfraujoch (See Figure 23). Our measurements allow to characterize the strong seasonal variation of C_2H_2, with maximum columns generally observed around mid-February. On average, the peak-to-peak amplitude amounts to nearly 90% of the mean yearly column.

As for HCN, the Jungfraujoch 7-15 km time series has been compared with ACE-FTS data. These latter correspond to an update of the standard version 2.2. Vertical profile

distributions are retrieved using 14 lines from both the MCT and InSb domains. Over northern mid-latitudes, vmr values are generally available from 17 km down to at best 7 km. Corresponding ACE-FTS partial columns can be compared to Jungfraujoch data, since the ground-based retrievals are sensitive to that range, as shown by the information content analysis.

Right frame of Figure 27 compares the Jungfraujoch and the ACE-FTS data sets. The latter includes all occultation measurements obtained between 41 and 51ºN latitude and extending down to 7 km. The Jungfraujoch time series (in blue) is characterized by a clear seasonal modulation, with partial columns ranging from about 1 to $9x10^{14}$ molec./cm^2. The Jungfraujoch and ACE-FTS data sets (in orange) agree reasonably well, although the latter seems to be slightly biased high, especially during summertime. An extension in time of the ACE-FTS data set is needed to confirm these first conclusions.

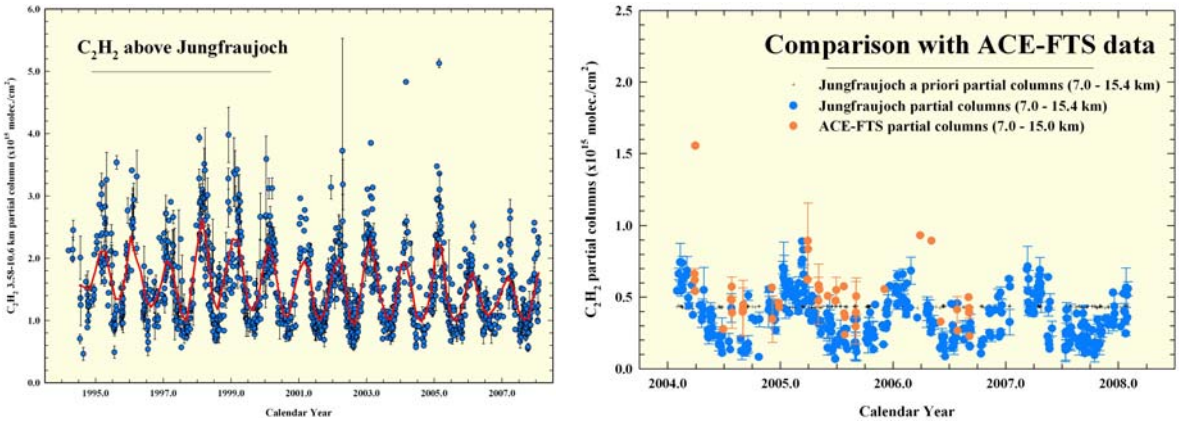

Figure 27: Timeseries of C_2H_2 above the Jungfraujoch and comparison with ACE-FTS data

7. Future work and perspectives

a. HCHO

- Procedures to detect and quantify HCHO from both FTIR and MAXDOAS spectra have been successfully developed and validated within this first phase of AGACC, at Uccle as well as at the Ile de La Réunion (21°S, 55°E).
- Our results tend to indicate that it will be difficult to measure H_2CO at the Jungfraujoch with the MAXDOAS instrument – because H_2CO levels are about a factor 10 lower. This will be verified during the second phase of AGACC.
- For the Jungfraujoch FTIR measurements, the specific experimental setup gives full satisfaction. Its routine use will allow to extend the HCHO observational data base. For the retrievals, we still want to evaluate the possible benefit from using additional microwindows compatible with our narrow optical filter, and to estimate the impact of the choice of the HCHO vertical distribution on the retrieved total columns.

b. HCN

- A successful strategy has been developed using Jungfraujoch observations; corresponding products have been characterized in terms of information content and associated errors and time series have been produced. More work is still needed to define a successful strategy to retrieve HCN from Reunion Island: this will be done in phase 2 of AGACC.
- Time series will be archived at the NDACC data center as soon as the new format is defined

- Correlation with C_2H_2, C_2H_6 and other biomass burning tracers will be performed in order to identify special events at the Jungfraujoch station. In such cases, retrievals of C_2H_4 will be performed.

c. $^{13}CH_4$ and CH_3D

- Complete time series of $^{13}CH_4$ and CH_3D will be generated using the strategies developed within AGACC
- The ratios of the isotopologues to the main methane isotopologue will be computed and analysed

d. C_2H_2

- Time series will be archived at the NDACC data center as soon as the new format is defined
- The new strategy will be tested using Reunion Island spectra

WP 1400: Feasibility studies

1. Ethylene (C_2H_4)

Ethylene originates from a variety of anthropogenic (e.g. cars in urban areas) and natural (e.g. plants, volcanoes, forest fires) sources. Due to its very short chemical lifetime, it's difficult to detect C_2H_4 from FTIR spectra, in particular at the high-altitude remote site of the Jungfraujoch. However, we have selected three microwindows and showed that it's possible to clearly detect larger absorptions of ethylene in FTIR spectra recorded during special events, e.g. under enhanced biomass burning. Due to the limited information content, it's only possible to derive vertical total columns of C_2H_4 from spectra recorded at very high SZA (between 85 and 90°). At such high SZA, spectra are usually recorded at a "reduced" resolution of 6.1 mK. Ethylene total abundances above ISSJ have been derived by using the SFIT-2 v3.91 algorithm and the HITRAN-2004 database. A realistic a priori VMR profile for ethylene has been constructed from data found in the "Spectroscopic Atlas in the middle Infra-Red", published by Meier et al. , 2004.

Figure 28 presents an example of detection of ethylene enhancement above ISSJ, using one of the three available microwindows. The blue curve shows a spectrum recorded at 89.8° with a strong absorption due to ethylene (see grey arrow) while the red curve reproduces an FTIR spectrum obtained under similar geometric conditions four days after, but corresponding to background atmospheric contents. A total column of 1.18 10^{15} molec./cm^2 was retrieved in the first case, i.e. about four times larger than the mean total column value of 2.64 10^{14} molec./cm^2 computed for 1998.

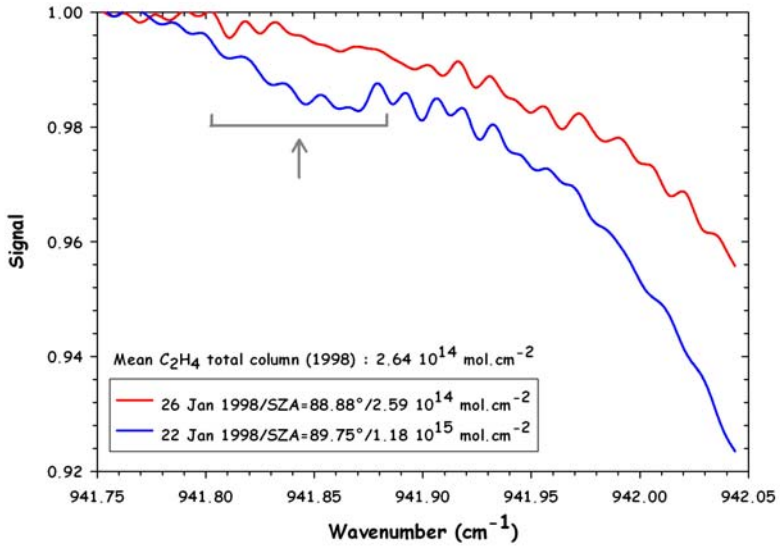

Figure 28: Comparison between spectra recorded under similar geometry and corresponding to C_2H_4 enhancement (blue curve, grey arrow) or normal conditions (red curve).

2. HCFC-142b

Other feasibility studies have been initiated, looking at absorptions of HCFC-142b (CH_3CClF_2) in Jungfraujoch low sun spectra. At present, microwindows encompassing HCFC-142b absorptions have been identified, they are located around 904, 967, 1134, 1192 and 1202 cm^{-1}. In all cases however, the absorptions are very weak, even in recent spectra, and there are several interferences by H_2O, CO_2, O_3, HNO_3, several CFCs, HCFC-22… that need to be carefully accounted for. Strategies using simultaneously several domains or even consecutive spectra at once are being tested to determine if reliable information on total columns of HCFC-142b can be derived from FTIR spectra. Conclusions of these analyses will be presented in the next yearly report.

3. Future work and perspectives for WP1400

We hope to be able to setup a robust approach to retrieve HCFC-142b from the Jungfraujoch station.

WP 2000 ACQUISITION AND EXPLOITATION OF SUPPORTING DATA

WP 2100: Laboratory spectroscopic measurements

WP 2110 : H_2O and isotopologues

During the phase 1, important progress was made concerning this WP. Linelists of HDO (11500-23000 cm^{-1}) and D_2O (8800-9520 cm^{-1}) have been generated and two papers have been published (Naumenko et al, 2006; Voronin et al., 2007). Also, the experimental linelists of HDO and D_2O that cover the wide 5600-11600 cm^{-1} region have been built. They contain line positions, intensities, self- and air-broadening coefficients, and air-induced shifts associated with their statistical uncertainties, and these results have been presented to several conferences (Carleer et al., 2006; Daumont et al. 2006, 2007a, 2007b; Jenouvrier et al., 2006a, 2006b; Fally et al., 2007). The complete rovibrational assignment process of these lines is ongoing and will lead to several publications once completed. In the near-IR spectral region (4200-6600 cm^{-1}), a complete linelist has been produced for the $H_2{}^{16}O$, $H_2{}^{17}O$, $H_2{}^{18}O$ and HDO isotopologues. It is accessible to the scientific community through the web

(http://www.ulb.ac.be/cpm) and a paper was published (Jenouvrier et al., 2006c). The region that will fill the gap between 6600 and 8800 cm^{-1} is under investigation, but requires great care due to strong congestion problems and to the simultaneous presence of the 3 isotopologues. This analysis has even been extended to 9250cm^{-1} because a better than previously signal-to-noise ratio could be obtained by using a different set-up during the last high resolution measurement campaign performed in collaboration with the Groupe de Spectroscopie Moléculaire et Atmosphérique (Université de Reims, France). The water vapor continuum underlying the discrete lines which has been recorded during high $H_2{}^{16}O$ pressure and temperature measurements is under investigation, but we are presently facing specific problems difficult to solve.

WP 2120 : $^{12}C_2H_2$

The planned activities for acetylene have been postponed to Phase 2. Indeed, this work is seeking to improve line intensities already accurate to 5 % (Mandin et al., 2000). In contrast with this, we showed in a recent contribution (Vander Auwera et al., 2007) that line intensities available in atmospheric databases, particularly HITRAN (Rothman et al., 2005) and GEISA (Jacquinet-Husson et al., 2008), for the 9 micron region of the formic acid spectrum (ν_6/ν_8 bands) were a factor of about 2 lower than laboratory measurements. The sharp *Q*-branch of the ν_6 band, located in an atmospheric window, is however commonly used to probe tropospheric formic acid by infrared remote sensing techniques. An improved set of line parameters was therefore urgently needed. Using results of our recent work (Vander Auwera et al., 2007), we therefore generated a new database for the 9 micron region of the formic acid spectrum. It includes a total of 49625 lines in the ν_6 and ν_8 bands of trans-$H^{12}C^{16}O^{16}OH$ with J" $\leq$ 79, Ka" $\leq$ 25, and lower and upper states energies up to 2700 and 4000 cm^{-1} respectively. Comparisons of low and high resolution laboratory spectra with spectra calculated at the same conditions using the new line list and HITRAN showed that the former provides a significantly improved and much more accurate description of the 9 micron region of the formic acid spectrum. An article describing this work is published (Perrin and Vander Auwera, 2007). The line list is now provided as an update to the HITRAN database (http://cfa-www.harvard.edu/HITRAN/) and will be included in the forthcoming version of GEISA.

WP 2130 : $^{13}C^{16}O$

We recorded absorption spectra of the 1–0 band of $^{13}C^{16}O$ near 2096 cm^{-1} using a Bruker IFS125HR high resolution Fourier transform spectrometer available at ULB. A high-purity commercial sample (Cambridge Isotopes Laboratories, 99% purity), at pressures ranging from about 40 to 260 Pa, was contained in a 1.46 cm long stainless steel cell, temperature stabilized at 296 K. Absolute line intensities were measured by adjustment of a synthetic spectrum to the observed spectrum of each line using a least squares fitting algorithm. Each line was given a Voigt profile. The instrumental effects arising from the truncation of the interferogram and the use of a 0.8 mm source aperture diameter were included as fixed contributions. We measured the absolute intensity of the P(20) to R(20) lines of the 1–0 band of $^{13}C^{16}O$, observed in the range 2008–2060 cm^{-1}. We estimated their accuracy to be about 2–3 %. Our results are on average 1.5 % higher than the intensity information available for these lines in the HITRAN database, characterized by a 2–5 % accuracy (Rothman et al., 2005). This is an excellent agreement, indicating that the accuracy of 1–0 band $^{13}C^{16}O$ line intensities in HITRAN is probably close to 2 %.

Prospects

Ongoing activities related to water vapor laboratory measurements will be carried on with the final aim to produce a comprehensive dataset covering the region 4600-23000cm^{-1}. The proposed work will address specifically 3 topics: the publication of HDO and D_2O assigned

linelists, the analysis of the region below 8800 cm^{-1}, the study of the underlying continuum. A future potential research could be the $H_2{}^{18}O$ and $H_2{}^{17}O$ isotopologues.
As already indicated in the report, the measurements of absolute line intensities in the ν_5 band of $^{12}C_2H_2$ observed near 729 cm^{-1}, initially planned for Phase 1, will be carried out during Phase 2. In addition, the line intensity measurements planned in the 5 to 10 micron region of the formaldehyde spectrum will be performed. The main difficulty to overcome is the accurate determination of the particle density of formaldehyde, unavailable through the measured total sample pressure because the gas phase is a mixture of the monomer with the more stable dimeric or trimeric forms. We hope that simultaneous line intensity measurements performed in the far infrared spectral region will give access to this necessary information.

WP2200 Ancillary geophysical and spectroscopic data

WP2300 Comparisons with complementary data

As seen in the above, our investigations have made use of ancillary and complementary data wherever useful. Comparisons have been made with satellite data, like GOME, SCIAMACHY, ACE-FTS, and IASI, whenever appropriate. Also the CIMEL aerosol data have supported the MAXDOAS and FTIR analyses at Uccle.

WP 3000 VALORISATION OF THE RESULTS

The results have been presented at many occasions at international Symposia, and at the yearly NDACC UV-Vis and Infrared Working Group Meetings, and a number of refereed publications have already appeared. We expect much benefit also from the COST Action WAVACS. The laboratory results have been or will be integrated in the international spectroscopic databases HITRAN and GEISA. Our expertise is also recognized through our participation to European projects like SCOUT-O3, GEOmon and HYMN. A list of publications and communications is presented hereinafter.
AGACC products have been or will be used in contributions to satellite validation; publications specifically related hereto have not been included in the list of publications below.

Peer reviewed publications

Baray, Jean-Luc, J. Leveau, S. Baldy, J. Jouzel, P. Keckhut, G. Bergametti, G. Ancellet, H. Bencherif, B. Cadet, M. Carleer, C. David, M. De Mazière, D. Faduilhe, S. Godin Beekmann, P. Goloub, F. Goutail, JM. Metzger, B. Morel, JP. Pommereau, J. Porteneuve, T. Portafaix, F. Posny, L. Robert and M. Van Roozendael, An instrumented station for the survey of ozone and climate change in the southern tropics, doi: 10.1039/b607762e, J. Environ. Monit., 8, 1-9, 2006.

Cheymol, A., H. De Backer, W. Josefsson, and R. Stübi, Comparison and validation of the aerosol optical depth obtained with the Langley plot method in the UV-B from Brewer Ozone Spectrophotometer measurements, J. Geophys. Res., 111, D16202, doi:10.129/2006JD007131, 2006.

Jenouvrier A., L. Daumont, L. Régalia-Jarlot, V. Tyuterev, M. Carleer, A. C. Vandaele, S. Mikhailenko, S. Fally, Fourier Transform measurements of water vapour line parameters in the 4200-6600 cm^{-1} region, J. Quant. Spectrosc. Radiat. Transfer,105, 326-355, 2006.

Naumenko O. V., O. Leshchishina, S. Shirin, A. Jenouvrier, S. Fally, A. C. Vandaele, E. Bertseva, A. Campargue, Combined analysis of high sensitivity Fourier transform and ICLAS-VeCSEL absorption spectra of D_2O between 8800 and 9520 cm^{-1}, J. Mol. Spectrosc., 238(1), pp79-90, 2006.

Neefs, E., M. De Mazière, F. Scolas, C. Hermans and T. Hawat, BARCOS an automation and remote control system for atmospheric observations with a Bruker interferometer, Rev. Sc. Instrum., 78, 035109-1 to -8, 2007.

Perrin A. and J. Vander Auwera, An improved database for the 9 μm region of the formic acid spectrum, J. Quant. Spectrosc. Radiat. Transfer 108 (2007) 363-370.

Reimann, S., M.K. Vollmer, D. Folini, M. Steinbacher, M. Hill, R. Zander and E. Mahieu, Observations of Long-Lived Anthropogenic Halocarbons at the High-Alpine site of Jungfraujoch (Switzerland) for Assessment of Trends and European Sources, Sci. Tot. Environ., 391, 224-231, 2008.

Rinsland, C.P., A. Goldman, J.W. Hannigan, S.W. Wood, L.S. Chiou and E. Mahieu, Long-term trends of tropospheric carbon monoxide and hydrogen cyanide from analysis of high resolution infrared solar spectra, J. Quant. Spectrosc. Radiat. Transfer, 104, 40-51, 2007.

Senten, C., M. De Mazière, B. Dils, C. Hermans, M. Kruglanski, E. Neefs, F. Scolas, A. C. Vandaele, G. Vanhaelewyn, C. Vigouroux, M. Carleer, P. F. Coheur, S. Fally, B. Barret, J. L. Baray, R. Delmas, J. Leveau, J. M. Metzger, E. Mahieu, C. Boone, K. A. Walker, P. F. Bernath, and K. Strong, Technical Note: Ground-based FTIR measurements at Ile de La Réunion: Observations, error analysis and comparisons with satellite data, Atmos. Chem. Phys. Discuss., 8, 827–891, 2008, 2008; accepted for publication in ACP.

Simon, P. C., M. De Mazière, M. Van Roozendael, and J-C. Lambert, An integrated approach to study the chemistry-climate interactions in the atmosphere, in Proceedings of the NATO Advanced Research Workshop on Remote Sensing of the Atmosphere for Environmental Security, Rabat, Morocco, 16-19 November 2005, A. Perrin, N. Ben Sari-Zizi, and J. Demaison (eds.), NATO Security through Science Series C: Environmental Security, Springer, 329-343, 2006.

Voronin B., Naumenko O. V., Carleer M., Coheur P.-F., Fally S., Jenouvrier A., Tolchenov R. N., Vandaele A. C., Tennyson J., Assignment of the HDO Fourier Transform absorption spectrum between 11500 and 23000 cm^{-1}. J. Mol. Spectrosc., 244, pp90-104, doi: 10.1016/j.jms.2007.03.008, 2007.

Zander, R., E. Mahieu, P. Demoulin, P. Duchatelet, G. Roland, C. Servais, M. De Mazière, S. Reimann and C.P. Rinsland, Our changing atmosphere: Evidence based on long-term infrared solar observations at the Jungfraujoch since 1950, *Sci. Total Environ., 391*, 184-195, 2008.

Not peer-reviewed publications

Cheymol, A., and H. De Backer, Impact of the aerosol particle concentrations on UV index prediction, European Geosciences Union General Assembly 2007, Vienna, (Austria), 15 – 20 April 2007.

Cheymol, A., H. De Backer, A. Mangold, R. Lemoine, A. Delcloo, J. Cafmeyer, and W. Maenhaut, Aerosol Optical Depth and Aerosol Characterisation in 2006 at Ukkel (Belgium), Proceedings of International Aerosol Conference, Saint Paul, USA, 10-15 September 2006.

De Mazière, M., C. Vigouroux, F. Hendrick, G. Vanhaelewyn, I. De Smedt, M. Van Roozendael, B. Dils, C. Hermans, M. Kruglanski, A. Merlaud, F. Scolas, C. Senten, M. Carleer, S. Fally, V. Duflot, J.M. Metzger, J.-L. Baray, R. Delmas, P. Duchatelet, Observations of halogens, CO, CH_4, and H_2CO at Ile de La Réunion from ground-based FTIR and MAXDOAS campaign measurements, poster presented at the "*4th general Assembly of SCOUT-O3*", 21-24 April 2008, Alfred Wegener Institute, Potsdam, Germany, 2008.

Dils, B., E. Mahieu, P. Demoulin, M, Steinbacher, B. Buchmann and M. De Mazière, Ground-based CO observations at the Jungfraujoch: comparison between FTIR and NDIR measurements, poster presented at the *"EGU 2008 General Assembly"*, 13 – 18 April 2008, Vienna, Austria, [Geophysical Research Abstracts, Vol. 10, EGU2008-A-08687], 2008.

Duchatelet, P., E. Mahieu, P. Demoulin, M. De Mazière, C. Senten, P. Bernath, C. Boone, K. Walker, Approaches for retrieving abundances of methane isotopologues in the frame of the AGACC project from ground-based FTIR observations performed at the Jungfraujoch, Poster presented at the European Geosciences Union General Assembly, Vienna (Austria), 15-20 April 2007, Vienna, Austria, [Geophysical Research Abstracts, Vol. 9, 06948], 2007.

Maenhaut, W., W. Wang, N. Raes, X. Chi, A. Cheymol, and H. De Backer, Atmospheric Aerosol Characterisation and Aerosol Optical Depth during 2006 at Ukkel, Belgium, Proceedings of IGAC, Cape Town, South Afrika, September 2006.

Mahieu, E., C. Servais, P. Duchatelet, R. Zander, P. Demoulin, M. De Mazière, C. Senten, K.A. Walker, C.D. Boone, C.P. Rinsland and P. Bernath, Optimisation of retrieval strategies using Jungfraujoch high-resolution FTIR observations for long-term trend studies and satellite validation, in Observing Tropospheric Trace Constituents from Space, ACCENT-TROPOSAT-2 in 2006-7, J. Burrows and P. Borrell, Eds., 280-285, 2007.

Mahieu, E., P. Duchatelet, P. Demoulin, C. Servais, M. De Mazière, C. Senten, C.P. Rinsland, P. Bernath, C.D. Boone, K.A. Walker, Retrievals of HCN from high-resolution FTIR solar spectra recorded at the Jungfraujoch station, poster presented at the European Geosciences Union General Assembly, Vienna (Austria), 15-20 April 2007, Vienna, Austria, [Geophysical Research Abstracts, Vol. 9, 07059], 2007.

Mahieu, E., P. Duchatelet, P.F. Bernath, C.D. Boone, M. De Mazière, P. Demoulin, C.P. Rinsland, C. Servais and K.A. Walker, Retrievals of C_2H_2 from high-resolution FTIR solar spectra recorded at the Jungfraujoch station (46.5ºN) and comparison with ACE-FTS observations, poster presented at the *"EGU 2008 General Assembly"*, 13 – 18 April 2008, Vienna, Austria, [Geophysical Research Abstracts, Vol. 10, EGU2008-A-08188], 2008.

Mahieu, E., R. Zander, P. Demoulin, P. Duchatelet, C. Servais, M. De Mazière, and C.P. Rinsland, FTIR Observations at the Jungfraujoch Station for Long-term Monitoring of the Troposphere and Validation of Space-based Sensors, in Measuring Tropospheric Trace Constituents from Space, ACCENT-TROPOSAT-2 in 2005-6, J. Burrows and P. Borrell, Eds., 274-277, 2007.

Senten,C., M. De Mazière, C. Hermans, B. Dils, A. Merlaud, M. Kruglanski, E. Neefs, F. Scolas, A.C. Vandaele, C. Vigouroux, K. Janssens, B. Barret, M. Carleer, P.-F. Coheur, S. Fally, J.L. Baray, J. Leveau, J.M. Metzger, E. Mahieu., Ground-based FTIR measurements at Ile de La Réunion: Observations, error analysis and comparisons with satellite data, Poster presented at the European Geosciences Union General Assembly,

Vienna (Austria), 15-20 April 2007, Vienna, Austria, [Geophysical Research Abstracts, Vol. 9, 08640], 2007.

Contributions at conferences

Carleer M., Clerbaux C., Coheur P.-F., Fally S., Hurtmans D., De Mazière M., Hermans C., Vandaele A. C., Daumont L., Jenouvrier A. (2006) Water, he said, Oral presentation at the ACE science team meeting, University of Waterloo, Ontario, Canada, Oct. 31-Nov. 3, 2006.

Cheymol, A., H. De Backer, Impact of the aerosol particle concentrations on UV index prediction, European Geosciences Union General Assembly, 2007

Cheymol A., De Backer H., Lam K.S., Kim J., Fioletov V., Siani A.M.,Vilaplana J.M.: Intercomparison of aerosol optical depth from Brewer Ozone Spectrophotometers and CIMEL sunphotometers measurements,submitted to Elsevier Science (2008)

Daumont L., A. Jenouvrier, L. Regalia-Jarlot, S. Fally, M. Carleer, C. Hermans, A. C. Vandaele, S. Mikhailenko, Fourier transform infrared spectroscopy of H2O, HDO and D2O: line parameters in the 5500-10800 cm-1 spectral region, Poster presented at The 20th Colloquium on High Resolution Molecular Spectroscopy, Dijon (France), September 3-7 2007.

Daumont L., A. Jenouvrier, S. Fally, C. Hermans, A. C. Vandaele, M. Carleer, Deuterium enriched water vapor Fourier transform spectroscopy: the 8800-10800 cm-1 spectral region, Oral presentation at the 62nd International Symposium on Molecular Spectroscopy, Columbus (Ohio, USA), 18-22 June 2007.

Daumont L., Jenouvrier A., Carleer M., Fally S., Vandaele A. C., Hermans C., HDO and D_2O long path spectroscopy: on-going work of the Brussels-Reims team, Oral presentation at The 9th HITRAN database conference, Cambridge (Ma, USA), 26-28 June 2006.

De Mazière, M., C. Vigouroux, F. Hendrick, G. Vanhaelewyn, I. De Smedt, M. Van Roozendael, B. Dils, C. Hermans, M. Kruglanski, A. Merlaud, F. Scolas, C. Senten, M. Carleer, S. Fally, V. Duflot, J.M. Metzger, J.-L. Baray, R. Delmas, P. Duchatelet, Observations of halogens, CO, CH4, and H2CO at Ile de La Réunion from ground-based FTIR and MAXDOAS campaign measurements, Poster presentation at the SCOUT-O3 Annual Meeting (Potsdam, April 21-24, 2008), 2008.

De Mazière, M., Cindy Senten, C. Vigouroux, B. Dils, M. Kruglanski, A.C. Vandaele, E. Neefs, F. Scolas, P.F. Coheur, M. Carleer, S. Fally, J. Leveau, FTIR observations at Réunion Island in support of ACE validation, oral presentation at the 14th ACE Science Team Meeting, Waterloo University, Oct. 30-Nov. 3, 2006.

De Mazière, M., Interpretation of FTIR observations, Invited lecture at the STAR International Research School: Atmospheric research in Suriname (Paramaribo, Suriname), March 13-17, 2006.

De Mazière, M., J.C. Lambert, and M. Van Roozendael, Integrated use of ground-based and satellite measurements of atmospheric composition, oral presentation at the International Scientific Conference in Celebration of the 75th Anniversary of the High Altitude Research Station Jungfraujoch, Interlaken, Switzerland (Congress Center Casino Kursaal), 11-14 September, 2006.

Dils, B., E. Mahieu, P. Demoulin, M. Steinbacher, B. Buchmann and M. De Mazière, Ground-based CO observations at the Jungfraujoch: Comparison between FTIR and NDIR measurements, Poster presentation at the EGU General Assembly (Vienna, April 13-18, 2008), 2008.

Dils, B., Ph. Demoulin, D. Folini, E. Mahieu, M. Steinbacher, B. Buchmann and M. De Mazière, Ground-based CO observations at the Jungfraujoch: Comparison between FTIR and NDIR in situ measurements, poster presentation by B. Dils at the 2nd ACCENT Symposium, Urbino, Italy, July 23-27, 2007.

Duchatelet, P., E. Mahieu, P. Demoulin, M. De Mazière, C. Senten, P. Bernath, C. Boone, K. Walker, Approaches for retrieving abundances of methane isotopologues in the frame of

the AGACC project from ground-based FTIR observations performed at the Jungfraujoch, Poster presented at the European Geosciences Union General Assembly, Vienna (Austria), 15-20 April 2007.

Fally S., Daumont L., Hermans C., Jenouvrier A., Vandaele A. C., Carleer, M., HDO and D_2O line parameters by Fourier Transform Infrared Spectroscopy: The 8800-11600 cm^{-1} spectral region, Poster presented at the European Geosciences Union General Assembly, Vienna (Austria), 15-20 April 2007.

Fally S., H. Herbin, P.-F. Coheur, M. Carleer, D. Hurtmans, C. Senten, M. De Mazière, C. Hermans, B. Dils, M. Kruglanski, A. Merlaud, F. Scolas, C. Vigouroux, J.-L. Baray, J.-M. Metzger, R. Delmas (2007) Ground-based and IASI satellite FTIR measurements of water vapour isotopologues above Ile de la Réunion, RiiS Reunion Island International Symposium, St-Gilles les Bains (Ile de la Réunion), 5-9 Nov. 2007.

Fally, S., P.-F. Coheur, M. Carleer, D. Hurtmans, M. De Mazière, C. Hermans, K. Janssens, M. Kruglanski, E. Neefs, F. Scolas, A.C. Vandaele, C. Vigouroux, B. Barret, J. Leveau, J.M. Metzger, Water vapour retrievals from ground-based FTIR observations at Ile de la Réunion: Focus on isotopologues, poster presentation by S. Fally at the EGU General Assembly, Vienna, Austria, 15-20 April 2007.

Jenouvrier A., Daumont L., Fally S., Carleer M., Vandaele A. C., Mikhailenko S. N., Starikova E. N., Long path FTS spectra of deuterated water vapour: new data for HDO molecule in the 8800-9100 cm^{-1} spectral region. Poster presented at the XV^{th} Symposium on High Resolution Molecular Spectroscopy, Nizhny Novgorod, 18-21 July 2006.

Jenouvrier A., Daumont L., Regalia-Jarlot L., Tyuterev Vl. G., Carleer M., Fally S., Vandaele A. C., Hermans C., Spectrométrie de la vapeur d'eau: mesures TF avec longs trajets d'absorption, Oral presentation at the Journées de Spectroscopie Moléculaire JSM, Lyon (France), 3-5 July 2006.

Jenouvrier A., Fally S., Vandaele A. C., Naumenko O. V., Leshchishina O., Shirin S. V., The Fourier transform absorption spectrum of the $D_2{}^{16}O$ molecule in the 10000-13200 cm-1 spectral region, Poster presented at the XVth Symposium on High Resolution Molecular Spectroscopy, Nizhny Novgorod, 18-21 July 2006, 2006b.

Kruglanski, M., M. De Mazière, A.-C. Vandaele, C. Hermans, B. Dils, G. Hermans, A. Joos de ter Beerst and A. Merlaud, Retrieval of formaldehyde from FTIR spectra: preliminary results, oral presentation (by M. De Mazière) at the NDACC IRWG, Puerta de la cruz, Tenerife, May 1-3, 2007.

Mahieu, E., P. Duchatelet, P. Bernath, C.D. Boone, M. De Mazière, P. Demoulin, C.P. Rinsland, C. Servais and K.A. Walker, Retrievals of C2H2 from high-resolution FTIR solar spectra recorded at the Jungfraujoch station and comparison with ACE-FTS observations, poster presentation at the EGU General Assembly (Vienna, April 13-18, 2008), 2008

Mahieu, E., P. Duchatelet, P. Demoulin, C. Servais, M. De Mazière, C. Senten, C.P. Rinsland, P. Bernath, C.D. Boone, K.A. Walker, Retrievals of HCN from high-resolution FTIR solar spectra recorded at the Jungfraujoch station, poster presented at the European Geosciences Union General Assembly, Vienna (Austria), 15-20 April 2007.

Perrin A. and J. Vander Auwera, An improved database for the 9 μm region of the formic acid spectrum, J. Quant. Spectrosc. Radiat. Transfer 108, 363-370, 2007.

Senten, C., M. De Mazière, C. Vigouroux, Data comparison: ground-based FTIR versus other sounders, results from a measurement campaign at Réunion Island, oral presentation at the STAR International Research School: Atmospheric research in Suriname (Paramaribo, Suriname), March 13-17, 2006.

Senten, C., M. De Mazière, C. Hermans, B. Dils, M. Kruglanski, A. Merlaud, E. Neefs, F. Scolas, A.C. Vandaele, C. Vigouroux, K. Janssens, B. Barret, M. Carleer, P.F. Coheur, S. Fally, J.L. Baray, J.M. Metzger, J. Leveau, E. Mahieu, Ground-based FTIR measurements at Ile de La Réunion: Observations, error analysis and comparisons with satellite data, poster presentation by C. Senten at the EGU General Assembly, Vienna, Austria, 15-20 April 2007.

Senten, C., M. De Mazière, C. Hermans, B. Dils, M. Kruglanski, E. Neefs, F. Scolas, A.C.

Vandaele, C. Vigouroux, K. Janssens, B. Barret, M. Carleer, P.F. Coheur, S. Fally, J.L. Baray, R. Delmas, J.M. Metzger, and E. Mahieu, Ground-based FTIR measurement campaigns at Ile de La Réunion: Campaign specifications, retrieval method and results, oral presentation at the Réunion Island International Symposium, St-Gilles, November 5-9th, 2007; submitted for publication in the Symposium Proceedings.

Van Malderen, R., Conference talk at KMI-IRM (12/12/2007), entitled 'Exploitation of radiosonde relative humidity measurements at Uccle'

Van Malderen, R., Oral presentation at the EGU 2008 (18/04/2008), entitled 'Trend analysis of the radiosonde relative humidity measurements at Uccle, Belgium'

Van Malderen, R., Poster presentation with title 'Exploitation of radiosonde relative humidity measurements at Uccle' at the MeteoClim symposium in Leuven (10/10/2007) (KMI-IRM)

Vander Auwera J., K. Didriche, A. Perrin and F. Keller, Quantitative spectroscopy of formic acid leading to an improved database in the 9 micron spectral region, The 20th Colloquium on High Resolution Molecular Spectroscopy, Dijon (France), September 3-7 2007.

Vander Auwera J., K. Didriche, A. Perrin, F. Keller, Absolute line intensities for formic acid and dissociation constant of the dimer, J. Chem. Phys. 126 (2007) 124311/1-124311/9.

Vigouroux, C., N. Theys, M. De Mazière, M. Van Roozendael, C. Senten, C. Hermans, M. Kruglanski, A.C. Vandaele, E. Neefs, F. Scolas, F. Hendrick, C. Fayt, S. Fally, M. Carleer, P.F. Coheur, and J. Leveau, Solar absorption FTIR and UV-visible MAXDOAS observations at the Ile de La Réunion, poster presentation at the SCOUT-O3 annual meeting (Zurich, Switzerland), March 20-24, 2006.

Vigouroux, C., M. De Mazière, M. Van Roozendael, I. De Smedt, B. Dils, F. Hendrick, C. Hermans, M. Kruglanski, A. Merlaud, E. Neefs, F. Scolas, C. Senten, S. Fally, M. Carleer, P.-F. Coheur, J.M. Metzger, J.-L. Baray, R. Delmas, P. Duchatelet, Observations of CH4, CH3D and H2CO at Ile de La Réunion from ground-based FTIR and MAXDOAS campaign measurements, poster presentation at the Réunion Island International Symposium, St-Gilles, November 5-9th, 2007; submitted for publication in the Symposium Proceedings.

Other valorisation activities

- S. Fally received the Young Scientists' Award in Spectroscopy, presented by the Journal of Quantitative Spectroscopy and Radiative Transfer, Elsevier, Sept. 2007
- AGACC meetings with partners:
    - Kick Off meeting, on 24/2/2006;
    - Progress meetings, on 13/11/2006 and 25/6/2007, attended by all partners, with invitation of members of Follow-Up Committee and representative of SPSDIII programme at Belgian Science Policy.
    - Meeting on water vapour measurements on the Plateau of Ukkel, on April 3, 2008.
- Participation to Kick-Off meeting of SPSDIII programme organized by Belgian Science Policy (Brussels, 26-27/3/2007)
- Development and maintenance of AGACC Web site at http://www.oma.be/AGACC/Home.html
- Redaction of AGACC fiches by coordinator, transmitted to Belgian Science Policy (February 2007)
- The measurement campaigns at Ile de La Réunion also deliver products to 3 European projects: SCOUT-O3 (http://www.ozone-sec.ch.cam.ac.uk/scout-o3), HYMN (http://www.knmi.nl/samenw/hymn), and GEOmon (http://www.geomon.eu). Team members of BIRA-IASB have participated to various working meetings in the frame of these projects.

- Participation in the Management Committee (KMI-IRM and ULB) and Working Groups (KMI-IRM, ULB and BIRA-IASB) of the COST action ES0604 Atmospheric Water Vapour in the Climate System (WaVaCS). This Action aims at integrating the research on water vapour and climate that is carried out in different areas (atmospheric monitoring, theory, modelling, and data assimilation).
- Short term scientific mission to Lindenberg Observatory, Deutscher Wetterdienst, in order to adopt Leiterer's correction method for vertical humidity profiles (R. Van Malderen, KMI-IRM).
- Supervision of Naïm Rahal, student master at SCQP-ULB (2006) : Stratégie d'inversion d'une distribution verticale des principaux isotopologues de la vapeur d'eau à partir de mesures FTIR sol: Mémoire présenté pour l'obtention du Grade légal de Licencié en Sciences Chimiques.
- Supervision of Valentin Duflot, student at the Université de La Réunion, who spent one months at BIRA-IASB (February 2008).
- Organisation of meetings :
  - Bruxelles, ULB, 09-10/03/2006: participants from SCQP-ULB, GSMA and IASB-BIRA.
  - Bruxelles ULB, 22-23/11/2006: same.
  - Bruxelles, ULB, 11-12/04/2007: same.
- Participation to the IUPAC project (International Union of Pure and Applied Chemistry) n°2004-035-1-100: "A database of water transitions from experiment and theory" (http://www.iupac.org/projects/2004/2004-035-1-100.html & http://theop11.chem.elte.hu/TG.htm) and to the related meetings (see below).
- Participation to meetings:
  - Boston, 28-29/06/2006: IUPAC meeting.
  - Bruxelles, IASB-BIRA, 04/09/2006: participants from SCQP-ULB, IASB-BIRA, and the Service d'Aéronomie de Paris VI, involved in the Canadian ACE (Atmospheric Chemistry Experiment) and French IASI (Infrared Atmospheric Sounding Interferometer) satellite projects.
  - Boston, 25/06/2006: meeting of the "HITRAN Advisory Committee".
  - Bruxelles, IASB-BIRA, 12/04/2007: IUPAC teleconference.
  - HITRAN committee meeting, Sunday 02/09/2007, Dijon, France
  - IUPAC Task group meeting, Friday 07/09/2007, Dijon, France
  - WAVACS (Atmospheric Water Vapour in the Climate System (WaVaCS COST action ES0604) kick-off meeting on Friday 05/10/2007 (participation of ULB and KMI).
  - Reims, France, Monday-Tuesday 03-04/12/2007: participants from ULB, GSMA, and Institute of Atmospheric Optics, Tomsk, Russia

- Lecturing: M. De Mazière, Ozon in al zijn facetten, Invited lecturer at the University of Antwerp, in the frame of the course Global Change in the education Milieuwetenschap, 2004, 2005, 2006, 2007

4 ANNEXES

4.1 REFERENCES

Barret B., De Maziere M.D., and Demoulin P.: Retrieval and characterization of ozone profiles from solar infrared spectra at the Jungfraujoch, J. Geophys. Res. 107(D24), 4788, doi:10.1029/2001JD001298, 2002.

Barret, B., D.Hurtmans, M. Carleer, M. De Mazière, E. Mahieu and P.-F. Coheur, Line narrowing effect on the retrieval of HF and HCl vertical profiles from ground-based FTIR measurements, J. Quant. Spect. Rad. Transfer, 95, 499-519, 2005.

Boone C. D. et al. Journal of Quantitative Spectroscopy and Radiative Transfer, 105, 525–532, 2007.

Cantrell, C.A., J.A. Davidson, A.H. McDaniel, R.E. Shetter, and J.G. Calvert: Temperature-Dependent Formaldehyde Cross Sections in the Near-Ultraviolet Spectral Region, J. Phys. Chem., 94, 3902-3908, 1990.

Clerbaux C. *et al.*, Space Research today (COSPAR info. bull. in Adv. SPace Res.), 168, 19-27, 2007.

De Smedt, I, J.F. Müller, T. Stavrakou, R. Van der A, H. Eskes, and M. Van Roozendael: Twelve years of global observation of formaldehyde in the troposphere using GOME and SCIAMACHY sensors, ACPD, Vol.8, pp. 7555-7608, 2008.

De Witte, S., Analysis of the solar radiation at Ukkel from a climate change point of view. Seminar 2 May 2007 at KMI.

Friess U., Monks P.S., Remedios J.J., Rozanov A., Sinreich R., Wagner T. and Platt U.: MAX-DOAS O4 measurements: A new technique to derive information on atmospheric aerosols: 2. Modeling studies, J. Geophys. Res. 111, D14203, doi:10.1029/2005JD006618, 2006.

Grainger J.F., and Ring J.: Anomalous Fraunhofer line profiles, Nature 193, 762,1962.

Greenblatt G.D., Orlando, J.J., Burkholder J.B., and Ravishankara A.R.: Absorption measurements of oxygen between 330 and 1140 nm, J. Geophys. Res. 95, 18577-18582, 1990.

Herbin, H., D. Hurtmans, S. Turquety, C. Wespes, B. Varret, J. Hadji-Lazaro, C. Clerbaux, and P.-F. Coheur, Global distribution of water vapour isotopologues retrieved from IMG/ADEOS data, Atmos. Chem. Phys., 7, 3957-3968, 2007

Holben B.N., Eck T.F., Slutsker I., Tanre D., Buis J.P., Setzer A., Vermote E., Reagan J.A., Kaufman Y.J., Nakajima T., Lavenu F., Jankowiak I., and Smimov A.: AERONET - A federated instrument network and data archive for aerosol characterization, Rem.Sens.Env. 66(I), 1-16, 1998.

Hurtmans D. et al., ASSFTS meeting, 2005; http://home.scarlet.be/dhurtma/ & dhurtma@ulb.ac.be

Irie H., Kanaya Y., Akimoto H., Iwabuchi H., Shimizu A., and Aoki K.: First retrieval of tropospheric aerosol profiles using MAXDOAS and comparison with lidar and sky radiometer measurements, Atmos. Chem. Phys. 8, 341-350, 2008.

Jacquinet-Husson N. et al., The GEISA spectroscopic database: Current and future archive for Earth and planetary atmosphere studies, J. Quant. Spectrosc. Radiat. Transfer 109 (2008) 1043-1059.

Jenouvrier A., L. Daumont, L. Rgalia-Jarlot, V. Tyuterev, M. Carleer, A. C. Vandaele, S. Mikhailenko, S. Fally, Fourier Transform measurements of water vapour line parameters in the 4200-6600 cm-1 region, J. Quant. Spectrosc. Radiat. Transfer 105, 326-355, 2006c.

Kuang, Z. et al., Geophys. Res. Lett., 30(7), 1372, 2003

Leiterer et al., J. Atmos. Oceanic. Technol., 22, 18-29, 2005.

Mandin J.-Y., V. Dana, C. Claveau, Line intensities in the $\upsilon 5$ band of acetylene $^{12}C_2H_2$, J. Quant. Spectrosc. Radiat. Transfer 67, 429-446, 2000.

Mayer B., and Kylling A.: Technical note: The libRadtran software package for radiative transfer calculations – description and examples of use, Atmos. Chem. Phys. 5, 1855-1877, http://www.atmos-chem-phys.net/5/1855/2005/, 2005.

Meier, A. et al., Spectroscopic Atlas of atmospheric microwindows in the middle infra-red, 2004

Meller, R., and Moortgat, G. K.: Temperature dependence of the absorption cross sections of formaldehyde between 223 and 323 K in the wavelength range 225 - 375 nm, J. Geophys. Res., 105(D6), 7089-7102, 10.1029/1999JD901074, 2000.

Miloshevich et al., J. Atmos. Oceanic. Technol., 21, 1305-1327, 2004.

Naumenko O. V., O. Leshchishina, S. Shirin, A. Jenouvrier, S. Fally, A. C. Vandaele, E. Bertseva, A. Campargue, Combined analysis of high sensitivity Fourier transform and ICLAS-VeCSEL absorption spectra of D_2O between 8800 and 9520 cm^{-1}, J. Mol. Spectrosc., 238(1) 79-90, 2006.

Neefs, E., De Mazière, M., Scolas, F., Hermans, C., and & Hawat, T.: BARCOS, an automation and remote control system for atmospheric observations with a Bruker interferometer, Rev. Sci. Instrum., 78, 035109-1 TO 8, 2007.

Notholt J. et al., JQSRT, 97(1), 112-125, 2006

Platt U., Differential optical absorption spectroscopy (DOAS), in Air Monitoring by Spectroscopic Techniques, vol. 127, pp. 27-83, John Wiley, Hoboken, N.Y., 1994.

Pougatchev, N. S. and Rinsland, C. P.: Spectroscopic study of the seasonal variation of carbon monoxide vertical distribution above Kitt Peak., J. Geophys. Res., 100, 1409-1416, 1995.

Rodgers, C. D.: Inverse methods for atmospheric sounding: Theory and Practice, Series on Atmospheric, Oceanic and Planetary Physics, Vol. 2, World Scientific Publishing Co., Singapore, 2000.

Rothman L. S. et al., The HITRAN 2004 molecular spectroscopic database, J. Quant. Spectrosc. Radiat. Transfer 96, 139-204, 2005.

Rozanov A., Bovensmann H., Bracher A., Hrechanyy S., Rozanov V., Sinnhuber B.-M., Stroh F., and Burrows J.P.: NO_2 and BrO vertical profile retrieval from SCIAMACHY limb measurements: Sensitivity studies, Adv. Space Res. 36, 846-854, doi:10.1016/j.asr2005.03.013, 2005.

Schneider M. et al, Atmos. Chem. Phys. Discuss., 8, 4977-5006, 2008

Schneider, M. et al., Atmos. Chem. Phys. Discuss., 5, 9493-9545, 2005

Senten, C., M. De Mazière, B. Dils, C. Hermans, M. Kruglanski, E. Neefs, F. Scolas, A. C. Vandaele, G. Vanhaelewyn, C. Vigouroux, M. Carleer, P. F. Coheur, S. Fally, B. Barret, J. L. Baray, R. Delmas, J. Leveau, J. M. Metzger, E. Mahieu, C. Boone, K. A. Walker, P. F. Bernath, and K. Strong, ACPD, Vol.8, pp. 827-891, 2008; accepted for publication in ACP.

Spurr R.J.D., Kurosu T.P., Chance K.V.: A Linearized discrete Ordinate Radiative Transfer Model for Atmospheric Remote Sensing Retrieval, J. Quant. Spectrosc. Radiat. Transfer 68, 689-735, 2001.

Spurr R.J.D.: Simulatinous derivation of intensities and weighting functions in a general preuso-spherical discrete ordinate radiative transfer treatment, J. Quant. Spectrosc. Radiat. Transfer 75, 129-175, 2002.

Suortti et al., J. Atmos. Oceanic. Technol., 25, 149-166, 2008.

Van Roozendael, M., Fayt, C., Lambert, J. C., Pundt, I., Wagner, T., Richter, A., and Chance, K.: Development of a bromine oxide product from GOME, in Proc. ESAMS'99, WPP-161, p. 543-547, 1999.

Voronin B., Naumenko O. V., Carleer M., Coheur P.-F., Fally S., Jenouvrier A., Tolchenov R. N., Vandaele A. C., Tennyson J., Assignment of the HDO Fourier Transform absorption spectrum between 11500 and 23000 cm^{-1}, J. Mol. Spectrosc. 244 (2007) 90-104.

Wagner T., Dix B., Friedeburg v.C., Friess U., Sanghavi S., Sinreich R., and Platt U.: MAX-DOAS O4 measurements: A new technique to derive information on atmospheric aerosols –Principles and information content, J. Geophys. Res. 109, D22205, doi:10.1029/2004JD004904, 2004.

Wittrock F., Oetjen H., Richter A., Fietkau S., Medeke T., Rozanov A., and Burrows J.P.: MAX-DOAS measurements of atmospheric trace gases in Ny-Alesund –Radiative transfer studies and their application, Atmos. Chem. Phys. 4, 955-966, 2004.

4.2 ACRONYMS, ABBREVIATIONS AND UNITS

ACCENT	Atmospheric Composition Change – the European NeTwork of excellence
ACE-FTS	Canadian Atmospheric Chemistry Experiment - Fourier Transform Spectrometer
AERONET	AErosol RObotic NETwork
AOD	Aerosol Optical Depth
BIRA-IASB	Institut d'Aéronomie Spatiale de Belgique - Belgisch Instituut voor Ruimte-Aëronomie – Belgian Institute for Space Aeronomy
CIMEL	CIMEL Sun photometer
CO	Carbon monoxide
CH_4	Methane
C_2H_4	Ethylene
DOFS	Degrees Of Freedom for Signal
DSCDs	Differential Slant Column Densities
ESAC II	Experimental Studies of Atmospheric Changes II
FTIR	Fourier Transform Infra-Red
FTS	Fourier Transform Spectrometer
gb	ground-based
GEISA	Gestion et Etude des Informations Spectroscopiques Atmosphériques
GPS	Global Positioning System
GSMA	Groupe de Spectrométrie Moléculaire et Atmosphérique
HCFC	Hydrochlorofluorocarbon
H_2CO	Formaldehyde (also appears as HCHO)
HCHO	Formaldehyde (also appears as H_2CO)
HCN	Hydrogen cyanide
HDO	Deuterium protium oxide or heavy water
HITRAN	High-resolution transmission molecular absorption database
ICLAS-VeCSEL	IntraCavity Laser Absorption Spectroscopy - Vertical External Cavity System Emitting Laser
InSb	Indium - Antimonide
IPCC	Intergovernmental Panel on Climate Change
IR	Infrared
IRWG	Infrared Working Group
ISSJ	International Scientific Station of the Jungfraujoch
IWV	Integrated Water Vapour
KMI-IRM	Koninklijk Meteorologisch Instituut – Institut Royal de Météorologie - Royal Meteorological Institute of Belgium
LIDORT	Linearized discrete ordinate radiative transfer
mK	milliKaiser (1 mK = 0.001 cm^{-1})
MAXDOAS	Multi-Axis Differential Optical Absorption Spectrometry
MCT	Mercury - Cadmium - Telluride
NDACC	Network for the Detection of Atmospheric Composition Change
N_2O	Nitrous oxide
NO_2	Nitrogen dioxide
O_3	Ozone

OCS	Carbonyl sulfide
OH	Hydroxyl radical
PTU	Pressure, temperature, relative humidity
RMS	root-mean-square
SCDs	Slant column densities
SCOUT-O3	Stratospheric-Climate Links with Emphasis on the Upper Troposphere and Lower Stratosphere
SFIT-2	a spectral inversion (retrieval) algorithm used in the NDACC IRWG community
SMO	Standard Mean Ocean Value
SZA	Solar zenith angle
TPW	Total Precipitable Water
UV-Vis	Ultraviolet - Visible
vmr(s)	volume mixing ratio(s)
SZA	solar zenith angle
WaVaCS	Atmospheric Water Vapour in the Climate System